Validation and characterization of an *Srcap* conditional knockout mouse

Karanveer Johal

A thesis submitted to the University of Ottawa
in partial fulfillment of the requirements for the
Master of Science in Biology

Department of Biology
Faculty of Science
University of Ottawa

Abstract

Neurodevelopment requires precise regulation of gene expression, and disruption of chromatin remodeling contributes to neurodevelopmental disorders. SRCAP mediates the deposition of histone variant H2A.Z into the genome. H2A.Z influences gene expression, thus regulating brain development. However, the function of SRCAP in neurodevelopment remains unexplored. Here, we investigated Srcap function using N2A cells and a cortex-specific *Srcap* knockout (KO) mouse. We found that knockdown of *Srcap* in N2A cells reduced H2A.Z deposition at candidate genes and disrupted H2A.Z dynamics during neuronal differentiation, thus impairing gene expression. *In vivo*, conditional deletion of two *Srcap* alleles resulted in reduced cortical thickness and ventricular and cortical area, as well as impaired progenitor specification and neuronal migration. Notably, mice lacking only one *Srcap* allele (cHet) exhibited altered anxiety-related and exploratory behaviours. Together, these findings identify Srcap as a critical regulator of cortical development and behaviour by controlling H2A.Z deposition.

Le développement neurologique nécessite une régulation précise de l'expression génétique, et la perturbation du remodelage de la chromatine contribue aux troubles du neurodéveloppement. SRCAP intervient dans le dépôt de la variante d'histone H2A.Z dans le génome. H2A.Z influence l'expression génétique, régulant ainsi le développement cérébral. Cependant, la fonction de SRCAP dans le développement neurologique reste inexplorée. Nous avons étudié la fonction de Srcap à l'aide de cellules N2A et d'une souris knockout (KO) spécifique du cortex. Nous avons découvert que l'inhibition de Srcap dans les cellules N2A réduisait le dépôt d'H2A.Z au niveau des gènes candidats et perturbait la dynamique d'H2A.Z pendant la différenciation neuronale,

altérant ainsi l'expression génique. In vivo, la délétion conditionnelle de deux allèles de *Srcap* a entraîné une réduction de l'épaisseur corticale et des zones ventriculaires et corticales, ainsi qu'une altération de la spécification des progéniteurs et de la migration neuronale. Il est à noter que les souris ne possédant qu'un seulallèle Srcap (cHet) présentaient des comportements anxieux et exploratories modifiés. Ensemble, ces résultats identifient Srcap comme un régulateur essentiel du développement cortical et du comportement en contrôlant le dépôt de H2A.Z.

Acknowledgements

This work would not have been possible without the continued support of my family. I would like to thank my parents for providing me with the opportunity to pursue higher education, believing in me, and pushing me to do better. My brothers who support and rely on me have also motivated me to push past what I thought I could have accomplished to where I am today. My greatest thanks go to my paternal grandmother, who raised me and instilled in me the values and virtues that have made me the person I am today. I will forever be grateful for my family, and I dedicate my thesis to them.

The contributions of Dr. Gilda Stefanelli to my research cannot be overstated. Her guidance has been a key contributor to my success as a researcher. She has taught me many aspects of research that go beyond the basic experimental protocols and has been my role model as a young researcher. She has always pushed me harder than I push myself and this has allowed me to grow into the researcher I am today. I will always be grateful to her and will keep her teachings with me for the rest of my career as a researcher.

Table of Contents

List of Tables

List of Figures

List of Abbreviations

NDD	Neurodevelopmental Disorder
RGP	Radial Glial Progenitors
VZ	Ventricular Zone
IPC	Intermediate Progenitor Cell
SVZ	Subventricular Zone
mESC	Mouse Embryonic Stem Cells
mNP	Mouse Neural Progenitors
SRCAP	Snf-2-Related CREB-binding protein Activator Protein
SRCAP-C	SRCAP Complex
CBP	CREB-Binding Protein
TF	Transcription Factor
ASD	Autism Spectrum Disorder
FHS	Floating-Harbor Syndrome
shRNA	Short Hairpin RNA
PBS	Phosphate-Buffered Saline
RA	Retinoic Acid
ChIP	Chromatin immunoprecipitation
OFT	Open Field Test
EPM	Elevated Plus Maze
OR	Object Recognition Test
TCS	Three Chamber Sociability Experiment

Statement of Contributions

Chapter 2: **Srcap loss alters H2A.Z-dependent and neuronal differentiation-related gene expression in N2A cells**

This chapter was published in Biochemistry and Cell Biology

Authors:

Karanveer S. Johal[1], Sandra A. Youssef[1], Samira M. Ibrahim[1], Lina A Dizon-Mapula[1], Isabella R. Galluzzo[1] & Gilda Stefanelli*[1]

Affiliations:

[1]Department of Biology, University of Ottawa, 30 Marie Curie, Ottawa ON Canada, K1N 6N5

*To whom correspondence should be addressed: gilda.stefanelli@uottawa.ca

Study Concept and Design……..Karanveer S. Johal

Gilda Stefanelli

Laboratory Work……Karanveer S. Johal

Sandra A. Youssef

Samira M. Ibrahim

Lina A. Dizon-Mapula

Isabella R. Galluzzo

Data Analysis……..…….Karanveer S. Johal

Manuscript Preparation……..……..Karanveer S. Johal

Gilda Stefanelli

Chapter 1: Introduction

1.1 Background

1.1.1 Neurodevelopmental disorders

Neurodevelopmental disorders (NDDs) are a group of conditions resulting from improper development of the nervous system[1]. They are characterized by impairments in cognition, behaviour, communication, learning, memory, self-control, and/or motor skills[2,3] that are evident in childhood and persist into adulthood. Data from the Ontario Brain Institute show that more than 300,000 children and youth in Ontario have been diagnosed with an NDD (https://braininstitute.ca/research-data-sharing/neurodevelopmental-disorders), with a worldwide prevalence placed around 13.4%[4]. While NDDs are becoming increasingly recognized due to rising attention to symptoms and better diagnostic processes[5], there is still much that is unknown about them; this is partially due to their complexity.

Genetic studies have identified a large and diverse set of risk genes associated with NDDs, highlighting extensive etiologic heterogeneity[6]. Importantly, many of these genes converge on shared biological pathways governing early brain development, including transcriptional regulation and regulation of chromatin states. This convergence suggests that disruption of fundamental developmental programs plays a central role in NDD pathogenesis. Consequently, understanding how gene expression is regulated during brain development and how these regulatory processes are disrupted is a critical step toward elucidating the biological mechanisms underlying NDDs.

1.1.2 NDDs and cortical development

The cerebral cortex underlies higher-order processes, including cognition, sensory integration, and voluntary behaviour, making its accurate development critical for normal neurological function.

Accordingly, substantial evidence indicates that defective cortical neurogenesis contributes to many forms of NDD[7,8].

Cortical development is a highly regulated process that relies on the tight spatial-temporal regulation of gene expression to control neural progenitor proliferation, differentiation into neurons and glia, and neuronal migration into the cortical layers. The neocortex is a six-layered structure composed of distinct regions that perform specific tasks[9]. Corticogenesis begins with a population of multipotent progenitors called radial glial progenitors (RGPs), which will give rise to all neuronal and glial lineages in the cortex[10]. Initially, RGPs expand via symmetric cell division to form a pool of cells that give rise to distinct neural lineages (Fig. 1)[11]. Proliferating RGPs form a layer of cells around the ventricles that is called the ventricular zone (VZ).

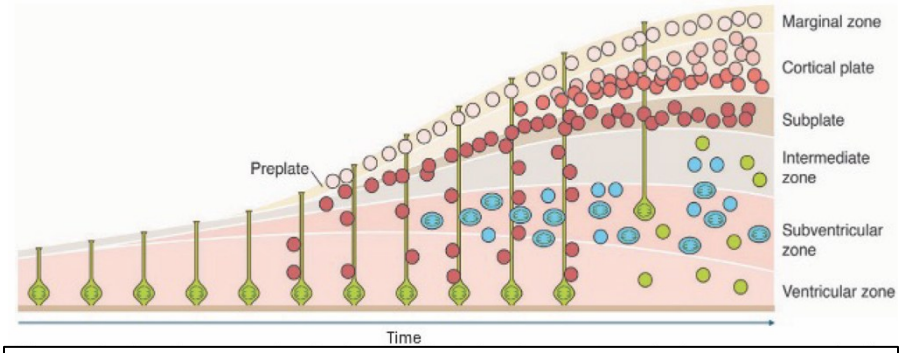

Figure 1: Corticogenesis. During cortical development, early born neurons (red) migrate radially to form the preplate. After, newly generated neurons migrate past earlier-born neurons to establish the cortical plate, splitting the preplate into the marginal zone and the subplate. Successive waves of neurogenesis generate cortical layers II-VI in an inside-out manner, with the marginal zone giving rise to layer I. Radial glial progenitors (RGPs) also generate intermediate progenitor cells (IPCs; blue) which migrate to the subventricular zone and undergo additional divisions to amplify neuronal output. After competition of neurogenesis, RGPs terminally differentiation into astrocytes (green). (Modified from Sanes et al., 2019).

This proliferation phase is followed by neurogenesis, during which neurons are generated. During this period, RGPs progressively transition from symmetrical to asymmetrical divisions. Initially, RGPs undergo direct neurogenesis, in which they divide to generate one RGP and one post-mitotic neuron. These early-born neurons contribute to the formation of the preplate (Fig. 1), the first neuronal layer of the developing cortex, which is subsequently reorganized as additional

waves of neurons are generated. As neurogenesis progresses, RGPs increasingly undergo indirect neurogenesis, producing one RGP and one intermediate progenitor cell (IPC). The IPC is a largely unipotent cell that migrates from the VZ to the inner subventricular zone (SVZ) and undergoes 1-2 rounds of symmetrical cell division to generate post-mitotic neurons. Indirect neurogenesis accounts for the majority of cortical neuron production and is a major driver of cortical expansion during development[12].

As later-born neurons migrate into the cortex, they split the preplate into two distinct layers: the marginal zone at the pial surface, which later persists as cortical layer I[13], and the subplate, a largely transient structure located beneath the developing cortex (Fig. 1). Neurons migrating between these two layers accumulate to form the cortical plate, which will give rise to cortical layers II–VI (Fig. 1)[14]. Continued neuronal production and migration result in the establishment of the six-layered neocortex in an inside-out manner, with earlier-born neurons occupying deeper layers and later-born neurons migrating past them to populate progressively more superficial layers. Consequently, layer VI is generated first, whereas layer II is generated last. Layer I, derived from the marginal zone, is an exception to this pattern: it is established early in development and remains the most superficial cortical layer[13]. Layer I provides molecular cues that regulate neuronal positioning and serves as the anchoring site for the basal (pial) projections of RGPs[15].

Neuronal migration occurs along the basal projections of RGPs, which function as a scaffold guiding neurons from their site of birth in the VZ or SVZ to their final laminar position[16] (Fig. 1). Individual cortical layers contain distinct neuronal subtypes that are generated within defined temporal windows and exhibit characteristic molecular and morphological features[17]. Each region of the neocortex is composed of all six layers, however, there are differences in the relative number of neurons from each layer in that region depending on the region's function.

Following neurogenesis, gliogenesis begins, and the RGPs start to generate glial cells. After gliogenesis, the remaining RGPs terminally differentiate into astrocytes. They lose their proliferative capacity and their attachment to the ventricular surface, migrate into the cortex, and then become multipolar[18].

1.1.3 The role of epigenetics in cell fate specification and cortical development

The progressive restriction of progenitor potential and the orderly generation of cortical cell types require mechanisms that not only initiate transcriptional programs but also stabilize them over developmental time. Early in corticogenesis, most neural progenitors are multipotent; however, as development proceeds, their developmental potential becomes progressively restricted[19]. This progressive restriction of fate underscores the necessity of tightly regulated temporal- and cell-type-specific gene-expression programs during corticogenesis. Together, these inputs bias progenitor cells toward specific developmental trajectories and stabilize differentiated cell identities. Although these transcriptional programs are genetically encoded, their activation and maintenance are governed by epigenetic mechanisms that regulate chromatin state and gene accessibility. Therefore, epigenetic mechanisms provide a molecular framework through which transient developmental cues can be converted into durable transcriptional states[20].

Consistent with their central role in neurodevelopment, mutations in numerous epigenetic regulators have been strongly associated with disrupted cortical development and an increased risk of NDDs[21]. Epigenetic mechanisms essential for cortical development include DNA methylation[22], histone modification[23], chromatin remodelling[24], and non-coding RNAs[25]. Together, these mechanisms act to establish, maintain, or restrict transcriptional states as neural progenitors transition toward differentiated identities.

1.1.4 Mechanisms of epigenetic regulation: the role of histone variants

Epigenetics refers to changes in DNA structure that do not alter its sequence. Chromatin provides the physical substrate upon which many epigenetic mechanisms act. This is a highly dynamic molecular structure composed of DNA associated with histone proteins. The fundamental unit of chromatin is the nucleosome, which consists of an octamer of histone proteins, two copies each of H2A, H2B, H3, and H4, around which approximately 147 base pairs of DNA are wrapped[26,27]. While nucleosome organization is essential for DNA compaction, it also creates a barrier to transcriptional machinery. Epigenetic mechanisms modulate this barrier by altering DNA-histone interactions or nucleosome positioning, thereby regulating chromatin accessibility and gene expression.

One of the most extensively studied epigenetic mechanisms is the post-translational modification of histone tails. These modifications can influence transcription either by directly altering the affinity between histones and DNA or by creating binding platforms for chromatin-associated proteins, ultimately altering chromatin structure and transcriptional output[28]. Rather than being static, epigenetic states are dynamically regulated by enzymatic "writers", "erasers", and "readers" that enable chromatin to respond to developmental signals while stabilizing appropriate gene expression programs[29].

While post-translational histone modifications modulate chromatin through reversible chemical marks, an additional layer of epigenetic regulation is achieved through the incorporation of histone variants. Histone variants are non-allelic counterparts to the canonical histones[30] that

confer distinct biochemical and structural properties to the nucleosome. They are present across all histone families, and their incorporation can alter nucleosome stability, chromatin accessibility, and regulatory potential[31]. Although variants have been implicated in various cellular processes, they are of particular interest in post-mitotic cells such as neurons, as their transcription is replication-independent, unlike that of canonical histones[30]. Histone variants regulate gene expression through multiple dynamic mechanisms, including histone variant exchange, turnover, and genomic relocation[32]. Variant exchange refers to the replacement of a canonical histone with a histone variant within a nucleosome (Fig. 2A). Variant turnover involves the removal and subsequent reincorporation of the same histone variant at a given genomic locus, thereby enabling continuous regulation of nucleosome composition (Fig. 2 B). Genomic relocation occurs when histone variants are removed from specific nucleosomes and redeposited at distinct genomic sites (Fig.3)[33].

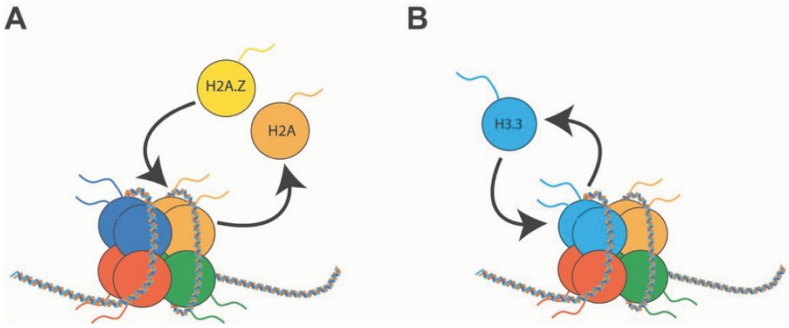

Figure 2: Histone variant dynamics. (A) Histone variant exchange: a canonical histone is removed from a nucleosome and is replaced by its variant. **(B)** Histone variant turnover: a histone variant is removed and then reincorporated. Both exchange and turnover are mediated by histone variant specific chaperones and RNA Pol II. (From Johal et al., 2023).

These dynamics are mediated by specialized and highly specific histone chaperones, often part of chromatin remodeling complexes, which control the selective deposition and removal of histone variants. In this context, histone chaperones function analogously to epigenetic “writers” and “erasers” by actively establishing or removing variants from nucleosomes, thereby dynamically shaping chromatin structure and transcriptional states.

1.1.5 H2A.Z and its chaperones in development

H2A.Z, a variant of histone H2A, has 60% amino acid similarity with H2A, including many of its core structural features[34], and the overall structure of nucleosomes containing H2A.Z is very similar to nucleosomes containing H2A. However, nucleosomes containing H2A.Z have weaker DNA binding, indicating that they can be more readily removed from chromatin[35]. H2A.Z is found in promoters and enhancers of active genes. However, H2A.Z has been described to have a role in the formation of heterochromatin, a tightly compact and transcriptionally silent form of chromatin.

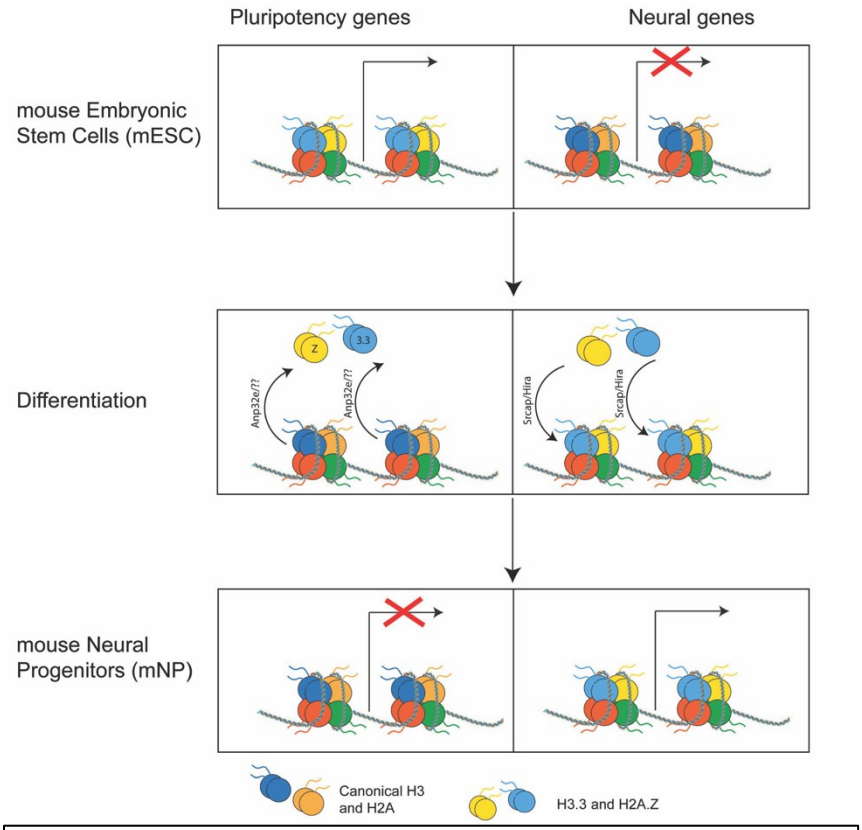

Figure 3: Histone variant genomic relocation. During differentiation of mouse embryonic stem cells (mESCs) into mouse neural progenitors (mNPs), H2A.Z is removed from pluripotency genes to inactivate them and incorporated into neural genes to activate them. (From: Johal et al., 2023).

These findings highlight how H2A.Z can act as either an active[37] or repressive[38] marker of transcription, depending on its location within the gene[38] and the post-translational modification on its tail[39,40].

The role of H2A.Z in development is suggested by the lethal outcomes of the knockout of *H2afz* (one of the genes encoding for H2A.Z), which in mice results in premature death[41] at embryonic day 7.5 (E7.5). Recent work has shown that H2A.Z and its chaperones are important regulators of gene expression during the initial stages of

neurodevelopment[8]. The ability of H2A.Z to regulate gene expression relies on its dynamic removal and reincorporation into chromatin[42–44]. Upon differentiation from mouse embryonic stem cells (mESC) to mouse neural progenitors (mNP), H2A.Z is lost at genes that become inactive and enriched at genes that become active in mNP (Fig. 3)[38,39]. This process is mediated by specific chaperones, whereby Anp32e acts as the "eraser" removing the variant[47,48], while Srcap acts as the "writer" of H2A.Z, mediating its deposition[49]. Impairment of the chaperones that regulate H2A.Z is detrimental. For instance, knockout of *Anp32e* in zebrafish leads to H2A.Z accumulation at Sox2 promoters and precocious induction of gastrulation[50]. Loss of *Srcap* in mESC results in loss of H2A.Z from the genome, de-repression of developmental genes and loss of stem cell identity[31]. This data implicates H2A.Z's dynamics in developmental processes.

1.1.6 The SRCAP Chromatin Remodelling Complex

SRCAP (Snf-2-related CREB-binding protein activator protein) encodes the ATPase core of a large chromatin remodelling complex: the SRCAP complex (SRCAP-C). ATP-dependent chromatin remodelling complexes regulate DNA accessibility by removing, incorporating, or altering nucleosome composition. There are four families of chromatin remodelling complexes which vary by their ATPase subunit that carry out specialized functions within cells: SWI/SNF, ISWI, CHD, and INO80 [51]. The SRCAP-C is part of the INO80 family of chromatin remodellers, which are involved in nucleosome editing by exchanging histone variants[52]. The primary function of the SRCAP-C is to exchange H2A for H2A.Z in nucleosomes. The SRCAP-C is highly conserved across eukaryotes, particularly in its core subunits and function,

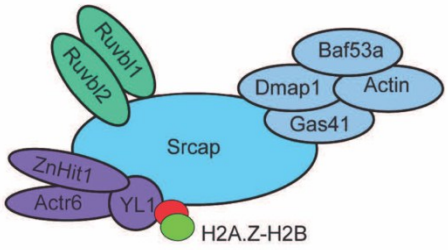

Figure 4: Composition of the SRCAP Complex. The SRCAP Complex is composed of multiple subunits organized into functional units around the SRCAP ATPase catalytic core.

whereas some accessory components and regulatory features diverge among species[53]. The core subunits of the SRCAP-C include the AAA+ ATPases RUVBL1 and RUVBL2, the actin-related protein ARP6, the H2A.Z-binding subunit YL1, and ZNHIT1, which together are required for ATP-dependent H2A.Z deposition (Fig. 4)[47].

The SRCAP-C is a potent transcriptional regulator linked to numerous developmental processes, including the maintenance of stem cell identity and renewal[31,55] and the differentiation into different lineages, such as neurons[56], muscle[57], and cardiomyocytes[58]. The SRCAP-C is enriched at nucleosome-depleted regions that flank the transcription start site[59]. It mediates the deposition of H2A.Z into the +1 nucleosome and creates a specialized promoter architecture that increases chromatin accessibility[37], facilitates transcription factor (TF) binding[33], and poises genes for rapid transcriptional activation[60]. The SRCAP-C also deposits H2A.Z in other regulatory regions, such as enhancers[61]. At active enhancers, H2A.Z deposited by SRCAP enhances RNA polymerase II recruitment, supporting enhancer activity and enhancer-promoter interaction[36]. Additionally, studies of lineage-specific chromatin landscapes show that H2A.Z pre-mark enhancers prior to activation, consistent with SRCAP-mediated deposition as part of establishing regulatory competence for future gene activation[62].

Mounting evidence supports the role of *SRCAP* in development through the regulation of H2A.Z. It was observed that *Srcap* null mice display lethality at E9.5[33], and knockdown of the *Srcap* homolog, *Domino*, in *Drosophila melanogaster* ovaries results in incomplete embryogenesis[63], indicating that Srcap is crucial for the early developmental programs. In mESC, loss of *Srcap* leads to reduced H2A.Z genomic levels, deregulation of developmental genes, and loss of stem cell identity[64]. Additionally, suppression of SRCAP prevents H2A.Z deposition and

restricts lineage commitment of myeloid progenitors[65]. These studies indicate that SRCAP mediates developmental gene expression by regulating H2A.Z incorporation across the genome.

1.1.7 SRCAP in Neurodevelopment and Human Disease

Mutations in *SRCAP* have been linked to the development of various NDDs, including autism spectrum disorder (ASD)[66], bipolar disorder[67], and ADHD[68]. SRCAP is also mutated in two rare disorders: Floating-Harbor Syndrome (FHS)[69], characterized by musculoskeletal abnormalities, microcephaly and severe to moderate intellectual disability, and DEHMBA (Developmental delay, Hypotonia-Musculoskeletal de fects, and Behavioural Abnormalities)[68], which differs from FHS for the presence of behavioural abnormalities like ADHD and schizophrenia (Fig. 5). There are several common neurodevelopmental features that are associated with SRCAP dysfunction, including language delay[70], intellectual disability[71], behavioural difficulties[68], and developmental delay such as delayed motor and learning milestones[68], highlighting the importance of SRCAP for normal neural development. Because *SRCAP* loss results in embryonic lethality[33], all known SRCAP mutations are heterozygous. Additionally, *SRCAP* lies within a susceptibility locus for neurodevelopmental disorders (16p11.2), with copy number variations in this locus often associated with ASD[72]. While human genetics clearly implicate SRCAP in neurodevelopment, the **mechanistic link between SRCAP-mediated chromatin remodelling and the observed neural**

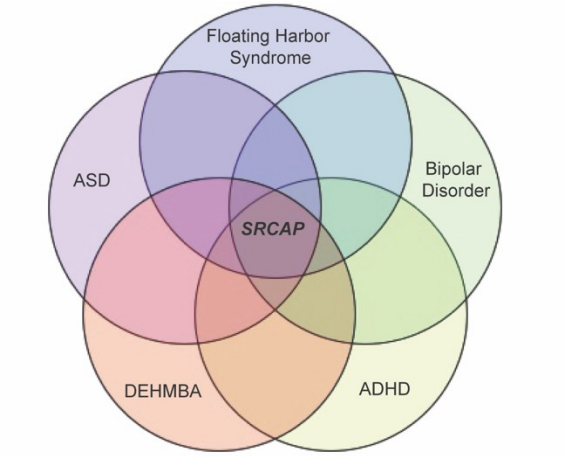

Figure 5: NDDs associated with SRCAP mutations. SRCAP dysfunction has been heavily associated with the presence of NDDs, including Floating-Harbor syndrome, bipolar disorder, ADHD, DEHMBA, and autism spectrum disorder.

and cognitive phenotypes remains poorly understood, motivating the use of model organisms to dissect its role during brain development.

1.1.8 Using a Mouse Model for Cortical Development

Though the human brain is larger and more complex than the mouse brain, mice are commonly used as a model in neuroscience. This is because the fundamental molecular and cellular mechanisms governing brain and cortical development are highly conserved between the two species[73]. As a result, mice have been extensively used to study cortical development and the genetic basis of NDDs. Many genes implicated in NDDs have historically been analyzed using transgenic mouse models, as these genes often perform similar functions in humans and mic[74]. For these reasons, a transgenic mouse model was generated for this study.

Cortical development follows a broadly conserved program in both humans and mice. In both species, cortical neurons are generated from RGPs, cortical layers are formed in an inside-out manner, and many of the transcription factors regulating neurogenesis and neuronal

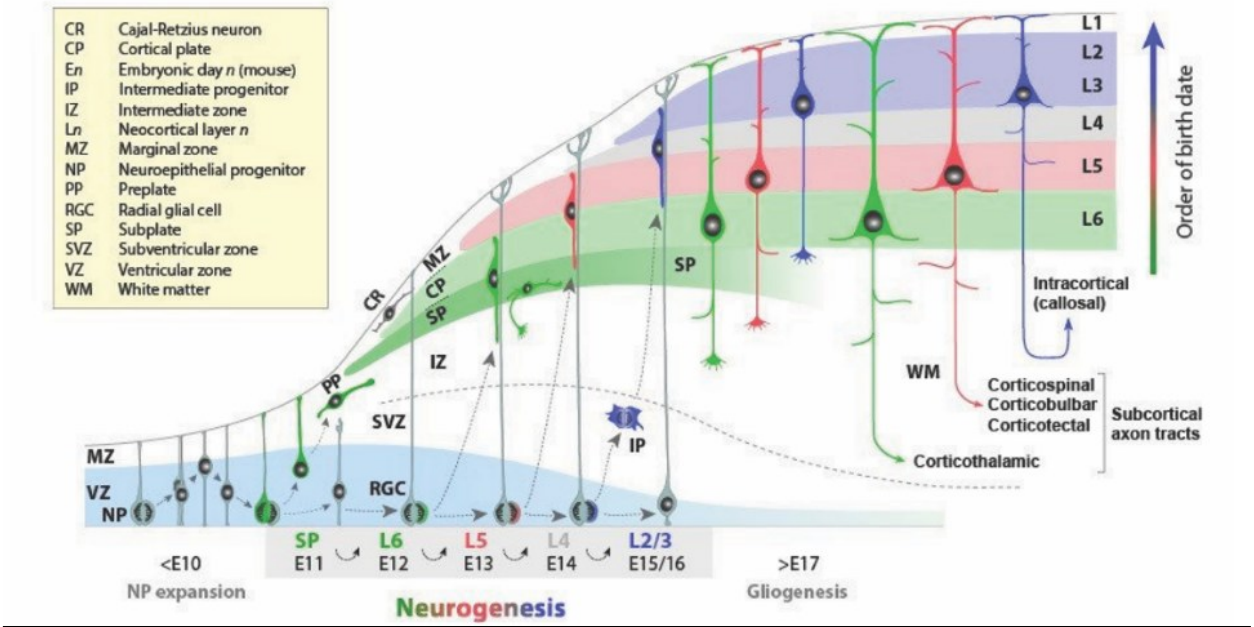

Figure 6: Cortical development in mice. Cortical neurogenesis in mice starts at E10.5 and neurons are generated until E17.7. Neurons keep migrating until P7 (From: Kwan et al. 2012).

differentiation are shared. However, notable differences exist, particularly in developmental timing and progenitor diversity. In humans, cortical development is a process that takes many months, beginning in the third week of gestation, and postnatal cortical maturation continues until early adulthood[75]. In mice, cortical development and maturation occur over a much shorter timeframe. Cortical development in mice begins at embryonic day 10.5 (E10.5), when the neuroepithelial cells of the neural tube transition into RGPs. The pool of RGPs undergoes rapid expansion at E10.5 and then gradually shifts from symmetric proliferative division to asymmetric division[76] from E10.5 to E11.5. Neurogenesis begins fully at E11.5 and continues until E17.5. Each day, a new population of neurons forms one of the 5 cortical layers in an inside-out fashion. After E17.5, gliogenesis begins, but neurons continue to migrate to reach their final position in the cortex until postnatal day 7 (P7) (Fig. 6)[42]. Another key difference between human and mouse cortical development lies in progenitor diversity. Despite these differences, the core processes of RGP-driven neurogenesis, neuronal migration, and cortical lamination are conserved.

Importantly, in both humans and mice, the functions and mechanisms of H2A.Z and Srcap are largely conserved. H2A.Z is evolutionarily conserved in all eukaryotes, and comparative studies have shown that H2A.Z from different species have a ~80% similarity at the amino acid level[77]. Additionally, H2A.Z is essential for early development for both humans and mice, with loss of H2A.Z resulting in embryonic lethality[41]. SRCAP is the vertebrate homolog of the yeast *SWR1* and the Drosophila *Domino*. The mechanism of using an ATP-dependent remodelling complex to exchange H2A for H2A.Z has been maintained from fungi to insecta to mammalia and indicates that the core mechanism was established early in evolution and retained in all eukaryotes[47,78].

Together, these findings support the use of mouse models to study SRCAP function during cortical development and provide a strong rationale for investigating SRCAP-mediated chromatin remodelling mechanisms in the developing mouse brain.

1.2 Knowledge Gap, Hypothesis, and Aims

While SRCAP has been implicated in general developmental processes and human genetic studies have linked *SRCAP* mutations to neurodevelopmental disorders, its role in neurodevelopment, particularly during cortical development and neuronal differentiation, has not been directly examined. Given Srcap's role in regulating H2A.Z incorporation, I hypothesized that **Srcap plays a fundamental role in brain development through the regulation of H2A.Z incorporation, and that impairment of this process undermines neurodevelopment, contributing to NDD etiology.** To test this hypothesis, this thesis is organized around three interconnected aims:

- **Aim 1**: Determine how Srcap regulates H2A.Z incorporation during neuronal differentiation and how its loss alters developmentally important gene expression programs.
- **Aim 2**: Examine the impact of Srcap loss during corticogenesis on neural progenitor specification and neuronal differentiation within the developing cortex.
- **Aim 3**: Assess whether disruption of Srcap-dependent chromatin regulation during cortical development leads to long-term behavioural alterations relevant to neurodevelopmental disorders.

1.3 References

1. Stefano Pallanti & Luana Salerno. Neurodevelopmental Disorders (NDDs): Beyond the Clinical Definition and Translational Approach. *Children (Basel)* **10**, 99 (2023).
2. Mullin, A. P. *et al.* Neurodevelopmental disorders: mechanisms and boundary definitions from genomes, interactomes and proteomes. *Transl Psychiatry* **3**, e329 (2013).
3. Deborah J Morris-Rosendahl & Marc-Antoine Crocq. Neurodevelopmental disorders-the history and future of a diagnostic concept. *Dialogues Clin Neurosci* **22**, 65–72 (2020).
4. Polanczyk, G., Salum, G., Sugaya, L., Caye, A. & Rohde, L. Annual research review: A meta-analysis of the worldwide prevalence of mental disorders in children and adolescents. *J Child Psychol Psychiatry* **56**, 345–365 (2015).
5. Cainelli, E. & Bisiacchi, P. Neurodevelopmental Disorders: Past, Present, and Future. *Children (Basel)* **10**, 31 (2022).
6. Leblond, C. *et al.* Operative list of genes associated with autism and neurodevelopmental disorders based on database review. *Mol Cell Neurosci* **113**, 103623 (2021).
7. Pietrobon, A., Yockell-Lelièvre, J., Flood, T. A. & Stanford, W. L. Renal organoid modeling of tuberous sclerosis complex reveals lesion features arise from diverse developmental processes. *Cell Rep* **40**, 111048 (2022).
8. Karanveer S Johal, Manjinder S Cheema, & Gilda Stefanelli. Histone Variants and Their Chaperones: An Emerging Epigenetic Mechanism in Neurodevelopment and Neurodevelopmental Disorders. *J Integr Neurosci* **22**, 108 (2023).
9. Ryan J Kast & Pat Levitt. Precision in the Development of Neocortical Architecture: from Progenitors to Cortical Networks. *Prog Neurobiol* **175**, 77–95 (2020).
10. P Malatesta, E Hartfuss, & M Götz. Isolation of radial glial cells by fluorescent-activated cell sorting reveals a neuronal lineage. *Development* **127**, 5253–63 (2000).

11. Li Cai, Nancy L Hayes, Takao Takahashi, Verne S Caviness Jr, & Richard S Nowakowski. Size distribution of retrovirally marked lineages matches prediction from population measurements of cell cycle behavior. *J Neurosci Res* **69**, 731–44 (2002).

12. Dhananjay Huilgol *et al.* Direct and indirect neurogenesis generate a mosaic of distinct glutamatergic projection neuron types in cerebral cortex. *Neuron* **111**, 2557–2569 (2023).

13. E C Gilmore & K Herrup. Cortical development: layers of complexity. *Curr Biol* **7**, R231-4 (1997).

14. Dan H. Sanes, Thomas A. Reh, William A. Harris, & Matthias Landgraf. *Development of the Nervous System*. (Academic Press, an imprint of Elsevier, London, 2019).

15. Xuejun Chai, Eckart Förster, Shanting Zhao, Hans H Bock, & Michael Frotscher. Reelin acts as a stop signal for radially migrating neurons by inducing phosphorylation of n-cofilin at the leading edge. *Commun Integr Biol* **2**, 375–77 (2009).

16. Stephen C Noctor *et al.* Dividing Precursor Cells of the Embryonic Cortical Ventricular Zone Have Morphological and Molecular Characteristics of Radial Glia. *J Neurosci* **22**, 3161–3173 (2002).

17. L C Greig, M B Woodworth, M J Galazo, H Padmanabhan, & J D Macklis. Molecular logic of neocortical projection neuron specification, development and diversity. *Nat Rev Neurosci* **14**, 755–69 (2013).

18. Arnold Kriegstein & Arturo Alvarez-Buylla. The glial nature of embryonic and adult neural stem cells. *Annu Rev Neurosci* **32**, 149–84 (2009).

19. Robert Beattie & Simon Hippenmeyer. Mechanisms of radial glia progenitor cell lineage progression. *FEBS Lett* **591**, 3993–4008 (2017).

20. Weinhold, B. Epigenetics: the science of change. *Environ Health Perspect* **114**, A160-7 (2006).

21. Zahir, F. & Brown, C. Epigenetic impacts on neurodevelopment: pathophysiological mechanisms and genetic modes of action. *Pediatr Res* **69**, 92R-100R (2011).

22. Dishu Huang, Wenjie Zhao, Hong Sun, Chen Yang, & Li Jiang. 5-mC DNA methylation in neurodevelopment: from molecular mechanisms to therapeutic implications. *Mol Biol Rep* **52**, 713 (2025).

23. Jisu Park, Kyubin Lee, Kyunghwan Kim, & Sun-Ju Yi. The role of histone modifications: from neurodevelopment to neurodiseases. *Signal Transfuct Target Ther* **7**, 217 (2022).

24. Britt Mossink, Moritz Negwer, Dirk Schubert, & Nael Nadif Kasri. The emerging role of chromatin remodelers in neurodevelopmental disorders: a developmental perspective. *Cell Mol Life Sci* **78**, 2517–2563 (2020).

25. Shuang-Feng Zhang, Jun Gao, & Chang-Mei Liu. The Role of Non-Coding RNAs in Neurodevelopmental Disorders. *Front Genet* **10**, 1033 (2019).

26. Bas van Steensel. Chromatin: constructing the big picture. *EMBO J* **30**, 1885–1895 (2011).

27. Benjamin Pierce. *Genetics: A Conceptual Approach*. (WH Freeman, 2005).

28. K Luger & T J Richmond. The histone tails of the nucleosome. *Curr Opin Genet Dev* **8**, 140–6 (1998).

29. Subhankar Biswas & C Mallikarjuna Rao 2. Epigenetic tools (The Writers, The Readers and The Erasers) and their implications in cancer therapy. *Eur J Pharmacol* **15**, 2–24 (2018).

30. Sara Martire & Laura A Banaszynski. The roles of histone variants in fine-tuning chromatin organization and function. *Nat Rev Mol Cell Biol* **21**, 522–541 (2020).

31. Talbert, P. & Henikoff, S. Histone variants at a glance. *J Cell Sci* **134**, jcs244749 (2021).

32. Wendy Wenderski & Ian Maze. Histone turnover and chromatin accessibility: Critical mediators of neurological development, plasticity, and disease. *Bioessays* **38**, 410–419 (2016).

33. Ye, B. *et al.* The chromatin remodeler SRCAP promotes self-renewal of intestinal stem cells. *EMBO J* **39**, e103786 (2020).

34. R K Suto, M J Clarkson, D J Tremethick, & K Luger. Crystal structure of a nucleosome core particle containing the variant histone H2A.Z. *Nat Struct Biol* **7**, 1121–4 (2000).

35. Naoki Horikoshi, Yasuhiro Arimura, Hiroyuki Taguchi, & Hitoshi Kurumizaka. Crystal structures of heterotypic nucleosomes containing histones H2A.Z and H2A. *Open Biol* **6**, 160127 (2016).

36. Brunelle, M. *et al.* The histone variant H2A.Z is an important regulator of enhancer activity. *Nucleic Acids Res* **43**, 9742–56 (2015).

37. Edwige Belotti *et al.* H2A.Z is dispensable for both basal and activated transcription in post-mitotic mouse muscles. *Nucleic Acids Res* **48**, 4601–4613 (2020).

38. Weronika Sura *et al.* Dual Role of the Histone Variant H2A.Z in Transcriptional Regulation of Stress-Response Genes. *Plant Cell* **29**, 791–807 (2017).

39. Anita A. Thambirajah *et al.* H2A.Z Stabilizes Chromatin in a Way That Is Dependent on Core Histone Acetylation. *J Biol Chem* **281**, 20036–20044 (2006).

40. Benedetto Daniele Giaimo, Francesca Ferrante, Andreas Herchenröther, Sandra B Hake, & Tilman Borggrefe. The histone variant H2A.Z in gene regulation. *Epigenetics Chromatin* **12**, 37 (2019).

41. R Faast *et al.* Histone variant H2A.Z is required for early mammalian development. *Curr Biol* **11**, 1183–1187 (2001).

42. Ku, M. *et al.* H2A.Z landscapes and dual modifications in pluripotent and multipotent stem cells underlie complex genome regulatory functions. *Genome Biol* **13**, R85 (2012).

43. Obri, A. *et al.* ANP32E is a histone chaperone that removes H2A.Z from chromatin. *Nature* **505**, 648–53 (2014).

44. Stefanelli, G. *et al.* The histone chaperone Anp32e regulates memory formation, transcription, and dendritic morphology by regulating steady-state H2A.Z binding in neurons. *Cell Rep* **36**, 109551 (2021).

45. Gorski, J. *et al.* Cortical excitatory neurons and glia, but not GABAergic neurons, are produced in the Emx1-expressing lineage. *J Neurosci* **22**, 6309–14 (2002).

46. Ding, C. *et al.* Srcap haploinsufficiency induced autistic-like behaviors in mice through disruption of Satb2 expression. *Cell Rep* **43**, 114231 (2024).

47. Ruhl, D. *et al.* Purification of a human SRCAP complex that remodels chromatin by incorporating the histone variant H2A.Z into nucleosomes. *Biochemistry* **45**, 5671–7 (2006).

48. Mao, Z. *et al.* Anp32e, a higher eukaryotic histone chaperone directs preferential recognition for H2A.Z. *Cell Res* **24**, 389–99 (2014).

49. Xiaoping Liang *et al.* Structural basis of H2A.Z recognition by SRCAP chromatin-remodeling subunit YL1. *Nat Struct Mol Biol* **23**, 317–23 (2016).

50. Tsai, H.-W., Grant, P. & Rissman, E. Sex differences in histone modifications in the neonatal mouse brain. *Epigenetics* **4**, 47–53 (2009).

51. Andrew Flaus, David M A Martin, Geoffrey J Barton, & Tom Owen-Hughes. Identification of multiple distinct Snf2 subfamilies with conserved structural motifs. *Nucleic Acids Res* **34**, 2887–905 (2006).

52. Sandipan Brahma *et al.* INO80 exchanges H2A.Z for H2A by translocating on DNA proximal to histone dimers. *Nat Commun* **8**, 15616 (2017).

53. Yunhe Bao & Xuetong Shen. INO80 subfamily of Chromatin Remodeling Complexes. *Mutat Res* **618**, 18–29 (2007).

54. Yangyang Feng, Yuan Tian, Zihan Wu, & Yanhui Xu. Cryo-EM structure of human SRCAP complex. *Cell Res* **28**, 1121–1123 (2018).

55. Jin, J. *et al.* In and out: histone variant exchange in chromatin. *Trends Biochem Sci* **30**, 680–7 (2005).

56. Funk, O., Qalieh, Y., Doyle, D., Lam, M. & Kwan, K. Postmitotic accumulation of histone variant H3.3 in new cortical neurons establishes neuronal chromatin, transcriptome, and identity. *Proc Natl Acad Sci U S A* **119**, e2116956119 (2022).

57. Stefanelli, G. *et al.* Learning and Age-Related Changes in Genome-wide H2A.Z Binding in the Mouse Hippocampus. *Cell Rep* **22**, 1124–1131 (2018).

58. Maze, I. *et al.* Critical Role of Histone Turnover in Neuronal Transcription and Plasticity. *Neuron* **87**, 77–94 (2015).

59. Madeline M Wong, Linda K Cox, & John C Chrivia. The chromatin remodeling protein, SRCAP, is critical for deposition of the histone variant H2A.Z at promoters. *J Biol Chem* **282**, 26132–9 (2007).

60. Elissa L Sutcliffe *et al.* Dynamic Histone Variant Exchange Accompanies Gene Induction in T Cells ▿ †. *Mol Cell Biol* **29**, 1972–1986 (2009).

61. Giho Park, Avinash B Patel, Carl Wu, & Robert K Louder. Structures of H2A.Z-associated human chromatin remodelers SRCAP and TIP60 reveal divergent mechanisms of chromatin engagement. *bioRxiv* **7**, 605802 (2024).

62. Ruben Boers *et al.* Retrospective analysis of enhancer activity and transcriptome history. *Nat Biotechnol* **41**, 1582–1592 (2023).

63. Ibarra-Morales, D. *et al.* Histone variant H2A.Z regulates zygotic genome activation. *Nat Commun* **12**, 7002 (2021).

64. Hsu, C.-C. *et al.* Recognition of histone acetylation by the GAS41 YEATS domain promotes H2A.Z deposition in non-small cell lung cancer. *Genes Dev* **32**, 58–69 (2018).

65. Ye, B. *et al.* Suppression of SRCAP chromatin remodelling complex and restriction of lymphoid lineage commitment by Pcid2. *Nat Commun* **8**, 1518 (2017).

66. Iossifov, I. *et al.* The contribution of de novo coding mutations to autism spectrum disorder. *Nature* **515**, 216–21 (2014).

67. Nishioka, M. *et al.* Systematic analysis of exonic germline and postzygotic de novo mutations in bipolar disorder. *Nat Commun* **12**, 3750 (2021).

68. Rots, D. *et al.* Truncating SRCAP variants outside the Floating-Harbor syndrome locus cause a distinct neurodevelopmental disorder with a specific DNA methylation signature. *Am J Hum Genet* **108**, 1053–1068 (2021).

69. Rebecca L Hood *et al.* Mutations in SRCAP, encoding SNF2-related CREBBP activator protein, cause Floating-Harbor syndrome. *Am J Hum Genet* **90**, 308–13 (2012).

70. Sarah M Nikkel *et al.* The phenotype of Floating-Harbor syndrome: clinical characterization of 52 individuals with mutations in exon 34 of SRCAP. *Orphanet J Rare Dis* **8**, 63 (2013).

71. Masaki Nishioka *et al.* Systematic analysis of exonic germline and postzygotic de novo mutations in bipolar disorder. *Nat Commun* **12**, 3750 (2021).

72. Lauren A Weiss *et al.* Association between microdeletion and microduplication at 16p11.2 and autism. *N Engl J Med* **358**, 667–75 (2008).

73. Goffinet AM. *Mouse Brain Development*. (Springer-Verlag, Berlin, 2000).

74. Zoltán Molnár *et al.* Comparative aspects of cerebral cortical development. *Eur J Neurosci* **23**, 921–34 (2006).

75. Joan Stiles. *The Fundamentals of Brain Development: Integrating Nature and Nurture*. (Harvard University Press, Brentwood, CA, USA, 2008). doi:10.2307/j.ctv1pncndb.

76. Kenneth Y. Kwan, N. Šestan, & E. Anton. Transcriptional co-regulation of neuronal migration and laminar identity in the neocortex. *Development* **139**, 1535–1546 (2012).

77. Joanna E Lowell, Franziska Kaiser, Christian J Janzen, & George A M Cross. Histone H2AZ dimerizes with a novel variant H2B and is enriched at repetitive DNA in Trypanosoma brucei. *J Cell Sci* **118**, 5721–30 (2005).

78. Francesca Mattiroli, Sheena D'Arcy, & Karolin Luger. The right place at the right time: chaperoning core histone variants. *EMBO Rep* **16**, 1454–66 (2015).

Chapter 2: Srcap loss alters H2A.Z-dependent and neuronal differentiation-related gene expression in N2A cells

This thesis section is a version of the following article:

Karanveer S. Johal, Sandra A. Youssef, Samira M. Ibrahim, Lina A. Dizon-Mapula, Isabella R. Galluzzo, Gilda Stefanelli. Srcap loss alters H2A.Z-dependent and neuronal differentiation-related gene expression in N2A cells. *Biochem Cell Biol* **103**, 1-12 (2025).

Srcap loss alters H2A.Z-dependent and neuronal differentiation-related gene expression in N2A cells

Karanveer S. Johal[1], Sandra A. Youssef[1], Samira M. Ibrahim[1], Lina A Dizon-Mapula[1], Isabella R. Galluzzo[1] & Gilda Stefanelli*[1]

[1]Department of Biology, University of Ottawa, 30 Marie Curie, Ottawa ON Canada, K1N 6N5

*To whom correspondence should be addressed: gilda.stefanelli@uottawa.ca

Journal: Biochemistry and Cell Biology

2.1 Abstract

The chromatin remodeler SRCAP plays a critical role in depositing the histone variant H2A.Z, which is essential for transcriptional regulation, chromatin accessibility, and neurodevelopmental processes. Despite its known importance, the mechanisms by which SRCAP regulates H2A.Z dynamics during neuronal differentiation remain poorly understood. Here, we investigated the impact of Srcap knockdown on H2A.Z incorporation and transcriptional regulation in N2A cells. Chromatin immunoprecipitation (ChIP) revealed reduced H2A.Z occupancy at activity-dependent and neurodevelopmental genes upon Srcap knockdown, confirming Srcap's role in H2A.Z deposition. Interestingly, CBP recruitment and global histone H3 acetylation were unaffected by Srcap knockdown at steady-state conditions, suggesting an H2A.Z-specific function of Srcap. We also observed that retinoic acid-induced neuronal differentiation leads to dynamic changes in H2A.Z levels at developmental loci, which are disrupted in Srcap-deficient cells. Gene expression analysis revealed altered expression of neurodevelopmental genes in the absence of Srcap, correlating with reduced H2A.Z occupancy. Together, these findings demonstrate that Srcap is essential for regulating H2A.Z dynamics and gene expression during neuronal differentiation, offering new insights into its role in chromatin remodelling and its potential involvement in neurodevelopmental disorders.

Keywords: histone variant, histone chaperone, H2A.Z, Srcap, cell differentiation, neurodevelopment

2.2 Introduction

The chromatin landscape plays a pivotal role in the regulation of gene expression, particularly during developmental processes, where precise spatiotemporal control of transcription is essential for proper cell differentiation and function[1]. Among the key modulators of chromatin structure are histone variants, which replace canonical histones in the nucleosome and confer unique regulatory properties[2]. H2A.Z, a highly conserved histone variant, is enriched at promoters and enhancers[3] and is implicated in transcriptional regulation, chromatin accessibility, and developmental processes[4]. In addition, H2A.Z has a prominent role in regulating higher brain functions like memory formation by regulating gene expression[5,6]. H2AZ's ability to regulate gene expression relies on its dynamic removal and reincorporation into chromatin, which is tightly regulated by specialized chaperones and remodelling complexes. These complexes, such as the SRCAP (SNF2-related CBP activator protein) complex, display high specificity for their histone variant. SRCAP is essential for depositing H2A.Z into nucleosomes at specific genomic loci[7–10]. It serves as the ATPase subunit of a large chromatin remodelling complex belonging to the family of INO80. The SRCAP complex (SRCAP-C) is a potent transcriptional regulator linked to numerous developmental processes, including the maintenance and renewal of stem cell identity[11,12] and differentiation into distinct lineages, such as neurons[13], muscle[14], and heart cells[15]. Mutations, knockdown, or knockout of SRCAP have been linked to global reductions in H2A.Z occupancy and transcriptional dysregulation[12,16,17]. However, in the context of the developing nervous system, where dynamic regulation of gene expression underpins processes such as neuronal differentiation, migration, and synapse formation, the role of SRCAP in modulating H2A.Z incorporation remains poorly understood. Moreover, while SRCAP has been shown to interact with transcriptional

coactivators such as CBP (CREB-binding protein)[18], its broader impact on CBP recruitment and histone acetylation is yet to be elucidated.

In this study, we investigate the role of SRCAP in regulating H2A.Z dynamics and transcriptional activity during neurodevelopment. Using N2A cells as a model for neuronal differentiation, we first examined the impact of Srcap knockdown on H2A.Z incorporation at loci critical for activity-dependent gene expression and neurodevelopmental pathways. We further assessed whether loss of Srcap affects CBP recruitment or histone acetylation. To understand how Srcap contributes to developmental gene regulation, we analyzed H2A.Z dynamics in response to retinoic acid (RA)-induced neuronal differentiation and evaluated gene expression changes in the absence of Srcap.

Our findings reveal that Srcap is indispensable for proper H2A.Z incorporation at both activity-dependent and developmental gene loci and that its absence disrupts H2A.Z dynamics during differentiation. Notably, Srcap loss does not impair CBP recruitment or histone acetylation, suggesting a specific role in regulating H2A.Z-dependent chromatin remodelling. These results provide new insights into the molecular mechanisms by which SRCAP influences chromatin architecture and gene expression during neurodevelopment, highlighting its potential relevance to neurodevelopmental disorders associated with SRCAP mutations.

2.3 Materials and Methods

2.3.1 Knockdown of *Srcap*

Knockdown of Srcap was achieved using a bicistronic vector containing a U6 promoter driving the expression of *Srcap* short hairpin RNA (shRNA), while GFP expression was driven by the CMV promoter. The following shRNA sequence for *Srcap* was employed:

GCCTTGATGGAACGGTTCAAT. A scrambled shRNA sequence expressing GFP was used as a control.

2.3.2 Cell Culture and Transfection

N2A cells were maintained in DMEM (Sigma–Aldrich, 11995-065) supplemented with 10% FBS, L-glutamine, 100 units/mL penicillin, and 100 µg/ml streptomycin, and incubated at 37°C with 5% CO_2. Cells were subcultured by first washing with 1X Phosphate-buffered saline (PBS) (Gibco 14190-136) and then incubating with 0.25% Trypsin (Gibco 15050-065) to detach the cells before splitting them into separate plates. Cells were transfected using LipofectamineTM 2000 (Life Tech., 52758) according to the manufacturer's instructions. Cells were collected or fixed 48-72 h post-transfection.

2.3.3 Differentiation with retinoic acid

To induce differentiation, 24 h after transfection, N2A media was replaced with a differentiation media consisting of DMEM with 1% FBS and 10 µmol/L retinoic acid (RA). For controls, the appropriate volume of DMSO was used instead of RA. New media with fresh RA was added every 24 h until the 72 h time point.

2.3.4 Chromatin immunoprecipitation (ChIP)

N2A cells were fixed on the plates with 1X PBS 1% formaldehyde for 5 minutes in an incubator at 37°C with 5% CO_2. Glycine was added to a final concentration of 125 mM at room temperature for 5 minutes. Media was removed and cells scraped and collected in ChIP lysis buffer (50 mmol/L Tris pH 8.1, 10 mmol/L EDTA, 1% SDS). Samples were subsequently sonicated using a Biorptor Plus sonicator for 30 cycles, 30 s on and 30 s off at 4°C. Every 10 cycles, the samples were removed, vortexed, and centrifuged to maintain homogeneity. Once the sonication was complete, the cell

debris was centrifuged at 13,800 XG for 5 min at 4℃. For each sample, 100 µl was used for ChIP diluted in 900 µl ChIP Dilution buffer (16 mmol/L Tris pH 8.1, 1.2 mmol/L EDTA, 0.01% SDS, 1% Triton, 170 mmol/L NaCl) and then treated with 20 µl of Protein G magnetic beads (Millipore, 16-662) and 1 µl of H2A.Z (Millipore, ABE1348), 1 µl of H3 (NEB, 2650S), or 1 µl of CBP (NEB, 7389S) overnight on rotator at 4℃. For each sample, 10 µl are kept as input and frozen at -80. The next day, ChIP samples were placed on a magnetic rack and washed sequentially with low-salt (20 mmol/L Tris pH 7.4, 0.1% SDS, 1% Triton X-100, 2 mmol/L EDTA, 150 mmol/L NaCl), high-salt (20 mmol/L Tris pH 7.4, 0.1% SDS, 1% Triton X-100, 1 mmol/L EDTA, 500 mmol/L NaCl), LiCl (10 mmol/L Tris pH8, 1% NP-40, 1% Sodium Deoxycholate, 1 mmol/L EDTA, 0.25 mol/L LiCl)), and TE (10 mmol/L Tris pH 7.4, 1 mmol/L EDTA) buffers, and incubated while rotating for 5 min between washes. Immune complexes were extracted using 100 µl TE Buffer and 0.5 µl proteinase K (Roche, 3115828001) for both ChIP and input samples and heated at 65 ℃ for 2 h, followed by 95 ℃ for 10 min before purification with PCR Purification Kit (Biobasic, BS664). Primers were designed to detect specific sequences. The ChIP data were calculated as percent input and then normalized to H3 and the control samples. The primer sequences are listed in Table 1.

Table 1. Primers used for qPCR with chromatin immunoprecipitation samples

Primer Name	**Primer Sequences**
Fos + 1	Forward-AGTGTCTACCCCTGGACCC Reverse-GCGTTGAAACCCGAGAACATC
Arc + 1	Forward-TGCCACACTCGCTAAGCTCC Reverse-AACTCCTCTGAGGCAGAAGCC
Nr4a2 + 1	Forward-CAGGAAGATAGCATCGCCCG Reverse-TGTGATTAGGGTCCCTCAGACT
Egr1 + 1	Forward-CTGCGTCCACCACGGG Reverse-CGAAGCTACTGAGGGCACAC
Sox5 + 1	Forward-CAGTCTACAAAAGGTGTGCGG Reverse-GTCTCCTCCGAGCTTACTGC
Fezf2 + 1	Forward-GGAGGGGAAGATGTTTGCCA Reverse-GGGAACTGGGCACTGAAAGA

2.3.5 RNA Extraction

RNA was extracted using the EZ-10 spin column total RNA extraction kit (BioBasic, BS82322) with an added DNase step (QIAGEN, 79254). The media was removed from the cells, and they were scraped in the lysis buffer provided in the EZ-10 total RNA extraction kit. After the RNA isolation complementary DNA was synthesized using high-capacity cDNA Reverse Transcription Kit (Applied BioSystems, 4368814). Primers designed in the lab were used to quantify the indicated transcripts, with data normalized to the geometric mean of β-actin and GAPDH. Primer sequences are listed in Table 2.

Table 2. Primers used for qPCR with cDNA samples

Primer Name	**Primer Sequences**
Gadph	Forward——GTGGAGTCATACTGGAACATGTAG Reverse——AATGGTGAAGGTCGGTGTG
ActB	Forward——AGATCAAGATCATTGCTCCTCCT Reverse——ACGCAGCTCAGTAACAGTCC
Sox5	Forward——TGCTTCAGCAACAGATCCAGG Reverse——CAGGGTAAGGGTCACTGCAC
Fezf2	Forward——GAAGTGTGCGGCAAGGTGTT Reverse——AGCTGCGATTGAAGGCTTTG
Arc	Forward——CTCTGCTCTTCTTCACTCGGTATG Reverse——GAGCTGAAGCCACAAATGC
Fos	Forward——GGCACTAGAGACGACAGAT Reverse——ACAGCCTTTCCTACTACCATTC
Egr1	Forward——GATAACTCGTCTCCACCATCG Reverse——AGCGCCTTCAATCCTCAAG
Nr4a2	Forward——GAGCGGACAAGGAGATCTGA Reverse——CAGTGTCGTAATTCAGCGAAGG

2.3.6 Western blotting

Transfected cells were washed with PBS (GIBCO, 14190-136) and scraped into 200 µl of 6X sample buffer (176 µl loading dye [6.6 ml 0.5M Tris pH 6.8, 3.4 ml glycerol, 1 g SDS, 0.1 g Bromophenol blue], 24 µl B-2 Mercaptoethanol [BioShop MER002]) per well. Samples were then boiled at 95℃ for 5 min, and 25 µl were loaded on the gel with 5 µl of protein ladder (Bio-

Rad,1610374). Proteins were separated on a 15% gel using SDS-PAGE. The gel box was filled with run buffer (1X Tris Glycine/SDS Buffer, BioRad 1610772) and then transferred for 1h at 0.4 amps to a PVDF membrane (Millipore, IPVH00010). The transfer box was filled with a transfer buffer (200 ml MeOH; 100 ml 10X Tris/Glycine Buffer, BioRad 1610771; 700 ml distilled water). Membranes were blocked in TBS-T containing 5% milk for 1hr at RT and then incubated with primary antibodies: pH3 (acetyl K9, K14, K18, K23, K27, abcam AB47915, 1:1000, overnight) and Tubulin (NEB 15115S, 1:10.000, 1 h). After washing, membranes were incubated with appropriate secondary antibody (Life Technologies, 12005869, 1:1000) for 1 h at RT. Detection was performed using a BioRad ChemiDoc, and image analysis was conducted with Fiji/Imagej (NIH).

Adult cortices were lysed in RIPA buffer and dounce homogenized with 10 strokes. The lysate was incubated 10 min on ice followed by centrifugation at 13,000 rpm 4 ºC. The Pierce BCA Protein Assay Kit (ThermoScientific, 23227) was used to determine protein concentrations. After adding loading dye, samples were heated at 70°C for 10 min and run on a 4-20% gradient gel and then transferred for 1.5h at 100V to a PVDF membrane (Millipore, IPVH00010). Membranes were blocked in TBS-T containing 5% milk for 1hr at RT and then incubated with primary antibodies: Srcap (Bioss BS-12119R1:500, overnight) and Tubulin (NEB 15115S, 1:10.000, 1 h). After washing, membranes were incubated with appropriate secondary antibody (Life Technologies, 12005869, 1:500) for 1 h at RT. Detection was performed using a BioRad ChemiDoc, and image analysis was conducted with Fiji/Imagej (NIH).

2.3.7 Statistical analyses

Analyses were conducted using GraphPad Prism, with independent-samples t tests for single-variable manipulations for two groups and two-way ANOVA for multiple-variable manipulations. When the omnibus test was significant, post hoc analyses were conducted with LSD post hoc or independent samples t-tests when appropriate. The number of replicates per group is stated in the figure legends, as is data representation. Significance was set at $p < 0.05$. Significant outliers were identified using Grubbs's test for outliers in GraphPad Prism.

2.4 Results

2.4.1 Knockdown of Srcap in N2A cells reduces H2A.Z occupancy at candidate genes

The knockdown, knockout, and mutations of *Srcap* have been linked to reduced H2A.Z occupancy *in vivo* and *in vitro*[14,16,19,20]. To verify if Srcap influences H2A.Z incorporation in our cell system, we generated plasmids encoding short hairpin RNA (shRNA) targeting *Srcap* (sh*Srcap*) or a scramble control (shScr) (Fig. 7A). Then, N2A cells were transfected with sh*Srcap* or shScr, and chromatin immunoprecipitation (ChIP) for H2A.Z was carried out 48 hours after transfection (Fig.7B). H2A.Z signal was normalized to H3 binding on the same loci to account for any possible changes in nucleosome occupancy. Importantly, no change in H3 occupancy was detected between sh*Srcap* and shScr controls (Supplementary Figure 1B-C). Consistent with findings in other cell types, knockdown of *Srcap* results in the loss of H2A.Z from the first nucleosome (+1 nucleosome) downstream of the transcription start site (TSS) of *Fos, Arc* and *Egr1* (Fig. 7C). These are known H2A.Z-bound genes and have a prominent role in activity-dependent gene expression and memory formation[5,21]. To understand if Srcap can regulate H2A.Z binding at developmental genes, we

tested H2A.Z occupancy at the +1 nucleosome of *Sox5*, *Nr4a2* and *Fezf2*. These genes play critical roles in brain development and neuron differentiation and contribute to complex neurodevelopmental processes required for proper brain structure and function. Notably, H2A.Z levels displayed a significant reduction at these neurodevelopmental genes (Fig. 7C). To understand whether H2A.Z reduction is limited to specific loci, we performed western blot analysis on transfected cells to test global H2A.Z protein levels. We found that Srcap knockdown results in significantly lower levels of H2A.Z (Supplementary Figure 1A), indicating that Srcap regulates H2A.Z globally.

Overall, these findings demonstrate that Srcap is essential for the regulation of H2A.Z occupancy at both activity-dependent and neurodevelopmental genes, highlighting its critical role in gene regulation during neuronal development.

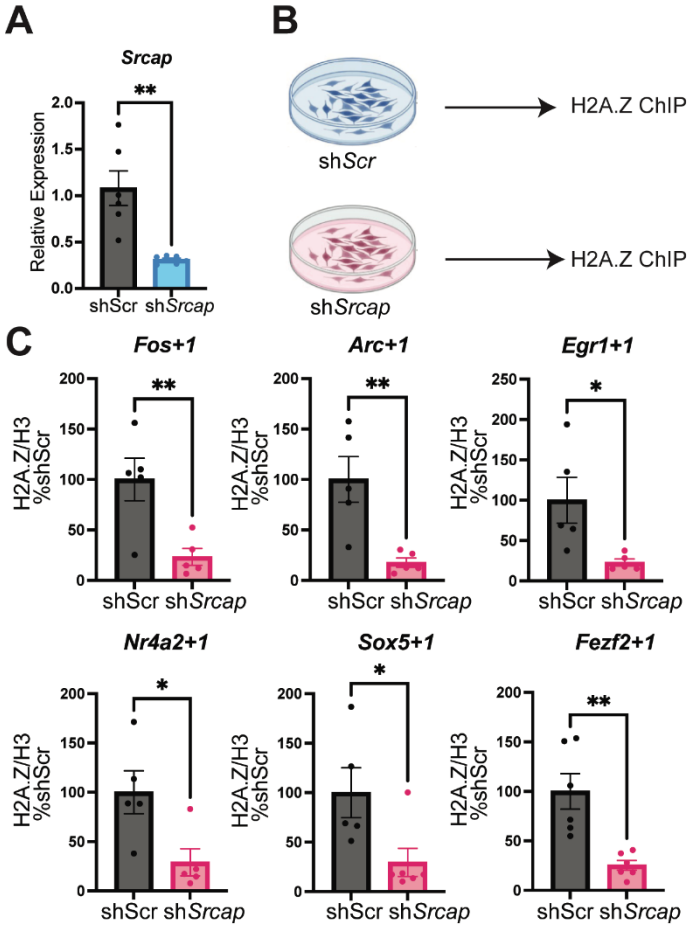

Figure 7: Knockdown of Srcap in N2A cells reduces H2A.Z abundance. (A) Quantitative PCR (qPCR) was used to assess the abundance of Srcap in Neuro2A (N2A) cells transfected with short hairpin Srcap (shSrcap) (n = 6) 48 hours transfection. Srcap abundance was normalized to short hairpin Scramble (shScr) transfection. The relative expression was normalized to housekeeping genes Gapdh and Actb. Data are expressed as mean ± SEM. **p ≤ 0.01. **(B)** Schematic representation of experimental workflow in cultured N2A cells. **(C)** ChIP was used to measure the occupancy of H2A.Z at the first nucleosome (+1 nucleosome) downstream of the transcription start site (TSS) in N2A cells 48 hours following transfection with shSrcap (n = 6). shSrcap transfection was normalized to shScr transfection. H2A.Z abundance is normalized to H3. Data are expressed as mean ± SEM. *p < 0.05.

2.4.2 Knockdown of *Srcap* in N2A cells does not interfere with CBP recruitment at H2A.Z-bound loci

Srcap was initially identified for its ability to bind Creb Binding Protein (CBP)[18], a histone acetyltransferase (HAT) with a prominent role in transcriptional activation[22]. Despite this, no data currently exists on CBP occupancy after the loss of Srcap. To test if Srcap is necessary to recruit CBP at H2A.Z binding sites, we first knocked down *Srcap* expression in N2A cells. 48 hours after transfection, we performed CBP ChIP (Fig.8A). CBP signal was normalized to H3 binding on the same loci to account for any possible changes in nucleosome occupancy. Interestingly, no changes in CBP binding were detected at genomic sites where we observed a reduction in H2A.Z (Fig. 8B), despite significant CBP enrichment being detected at the tested loci (Supplementary Figure 2).

CBP primarily exerts its functions by mediating H3 acetylation. To test for any potential loss in global H3 acetylation upon loss of Srcap, we transfected N2A cells with shScr and sh*Srcap* and performed western blotting on protein extracts. We used an antibody that recognizes multiple acetylated residues (acetyl K9, K14, K18, K23, K27, see materials and methods), including lysine residues 14, 18 and 23 that are commonly acetylated by CBP and its homolog p300[23,24]. Notably, no changes in global H3 acetylation were detected upon loss of Srcap (Fig. 8C).

These findings strongly suggest that Srcap functions regarding H2A.Z are independent of its role in recruiting CBP.

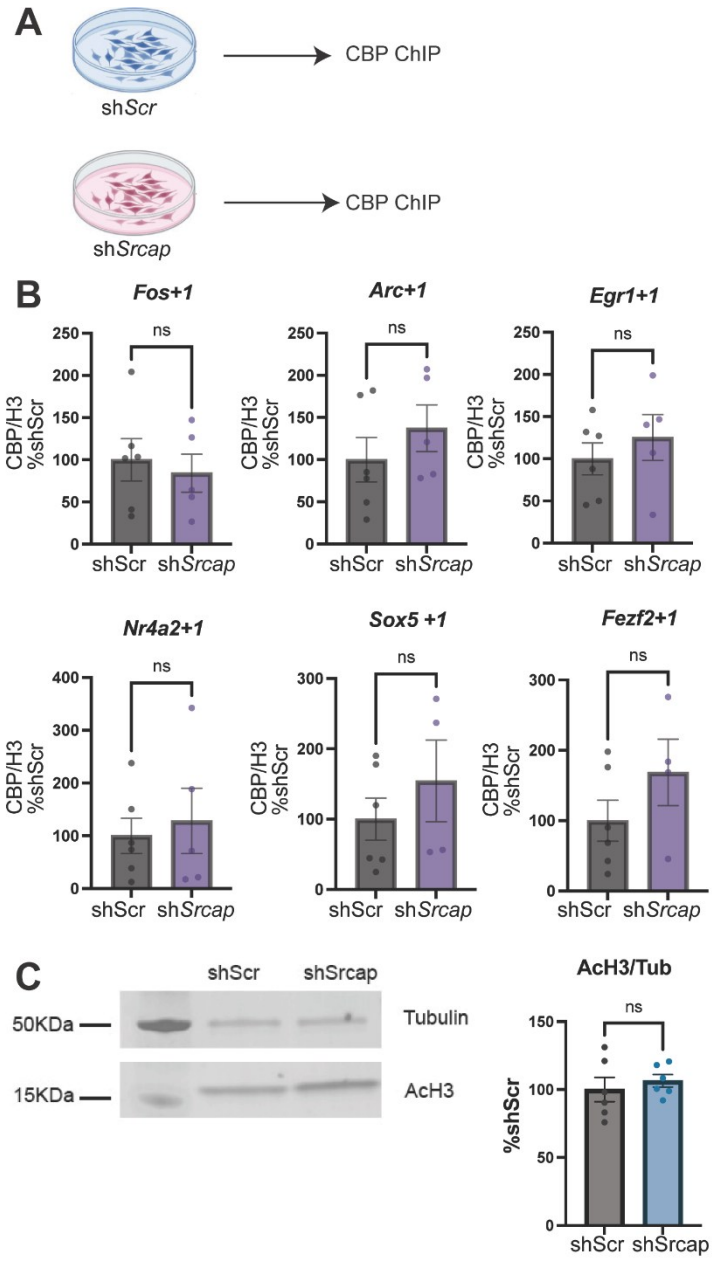

Figure 8: Knockdown of Srcap in N2A cells does not alter CBP chromatin levels. (A) Schematic representation of experimental workflow in cultured N2A cells. **(B)** ChIP was used to measure the abundance of CBP associated with chromatin in N2A cells 48 hours following transfection with shSrcap (n = 6). shSrcap transfection was normalized to shScr transfection. CBP abundance is normalized to H3. T-test *p < 0.05. **(C)** Western Blot was used to assess levels of acetylated H3 (AcH3) in N2A cells 48 hours following transfection with shSrcap (n = 3). shSrcap transfection was normalized to shScr transfection. AcH3 abundance is normalized to Tubulin. Data are expressed as mean ± SEM. *p < 0.05.

2.4.3 H2A.Z displays altered dynamics during N2A RA-induced differentiation in the absence of *Srcap*

H2A.Z is known to undergo activity-dependent removal during neuronal depolarization, which correlates with increased gene expression[5,6,21]. However, its dynamics during neurodevelopment remain unclear. To investigate H2A.Z dynamics during neuronal differentiation, we exploited the

ability of N2A cells to differentiate into neuronal-like cells following retinoic acid (RA) treatment. Cells were transfected with sh*Srcap* and shScr, and 24 hours after transfection, RA was added to the media (Fig. 9A). We collected cells for ChIP analyses 24- and 72-hours following RA treatment (Fig. 9A).

At 24 hours, control (shScr) cells showed a reduction in H2A.Z levels at activity-dependent (*Fos, Arc, Egr1*) and neurodevelopmental (*Nr4a2, Sox5, Fezf2*) genes, compared to DMSO-treated controls (Fig. 9B). However, Srcap knockdown abolished this decrease (Fig. 9B), preventing a significant reduction in H2A.Z levels. Notably, increased H3 occupancy was observed 24 hours after RA treatment in both shScr and sh*Srcap* cells (Supplementary Figure 3B). This suggests that the reduction in H2A.Z levels in shScr following RA may result from increased nucleosome occupancy rather than active H2A.Z removal. This effect may not be detectable in sh*Srcap* cells due to their already low H2A.Z levels. Importantly, when H3 is not considered and normalization is performed using %shScr DMSO, a significant reduction in H2A.Z is still observed at all tested loci following RA treatment in shScr but not in sh*Srcap* cells (data not shown). This indicates that active removal of H2A.Z may still be happening at the tested promoters and is impaired when Srcap is knocked down.

72 hours after RA treatment, a reduction in H2A.Z at the +1 nucleosome of H2A.Z genes *Fos*, *Arc* and *Egr1* was still observed (Fig. 9C). On the contrary, developmental genes *Nr4a2*, *Sox5* and *Fezf2* did not display a significant reduction (Fig. 9C). Importantly, sh*Srcap*-treated cells displayed an overall reduction in H2A.Z levels but no differences following RA treatment (Fig. 9C). Interestingly, we observed increased H3 occupancy following sh*Srcap* treatment at this time-point (Supplementary Figure 3C - 96 h post-transfection) that we did not observe in our previous experiments (Supplementary Figure 1 - 48 h post-transfection and 3B - 48 h post-transfection).

This suggests that compensatory mechanisms may be triggered by Srcap knockdown, thereby affecting nucleosome density.

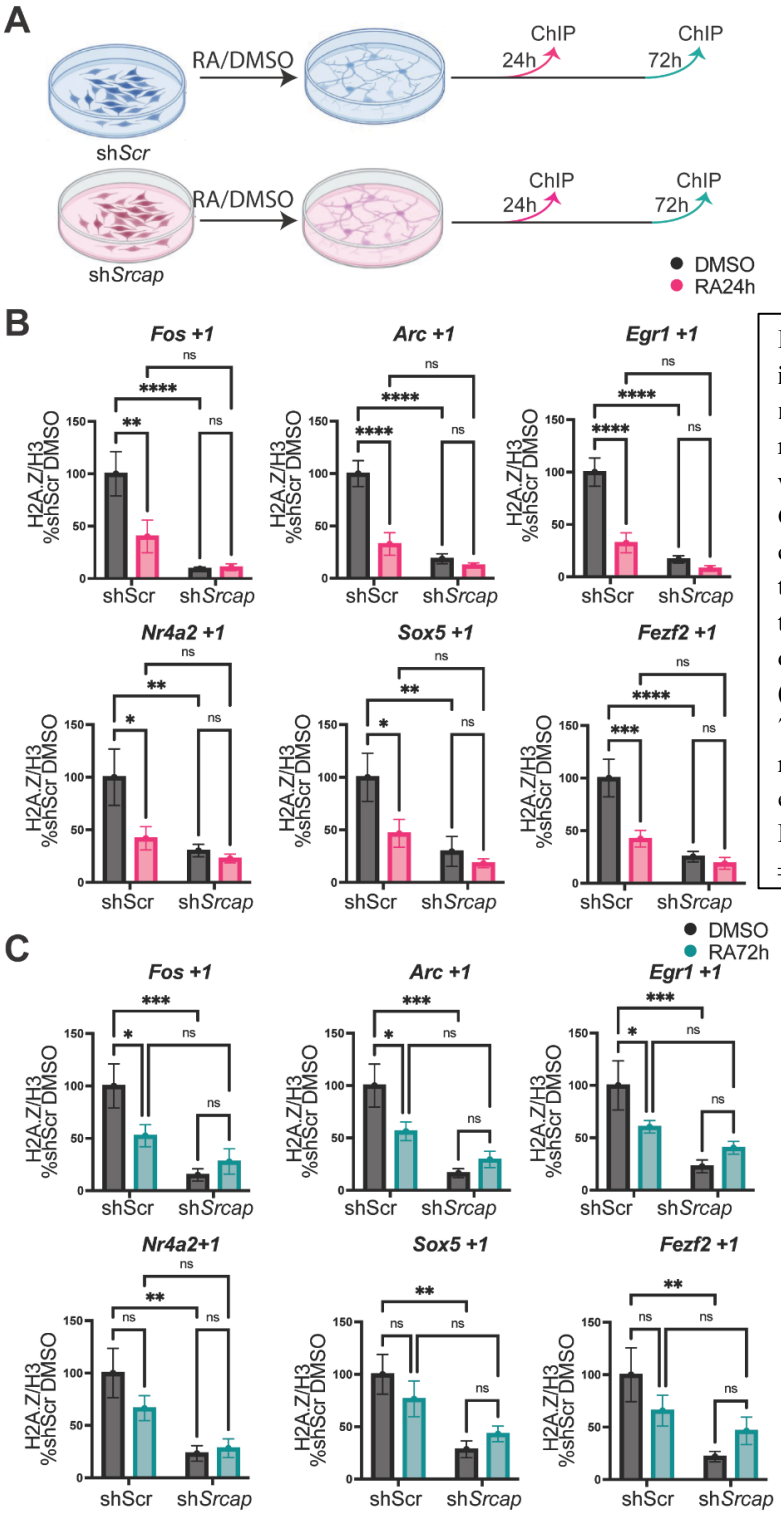

Figure 9: Knockdown of Srcap impairs differentiation-mediated reduction of H2A.Z. (A) Schematic representation of experimental workflow in cultured N2A cells. **(B-C)** ChIP was used to measure the change in the occupancy of H2A.Z at the +1 nucleosome of N2A cells transfected with shSrcap and differentiation with retinoic acid (RA) for **(B)** 24 hours (n = 6) or **(C)** 72 hours (n = 6). H2A.Z abundance is normalized to H3, and data are expressed as % compared to shScr DMSO. Data are expressed as mean ± SEM. Two-way ANOVA *p <

Given the differences in dynamics at developmental genes between 24 and 72 hours, we plotted the data to compare H2A.Z levels normalized to H3 after 24 and 72 hours of RA treatment (Fig. 10B). First, we plotted data relative to DMSO controls to determine whether our analysis could be influenced by extended time in culture or nucleosome density (Supplementary Figure 4). Notably, DMSO data revealed an overall reduction in H2A.Z levels in *Srcap*-depleted cells compared to shScr-treated cells (Supplementary Figure 4B) despite the increased H3 occupancy at 72h DMSO (Supplementary Figure 3C). Notably, we did not detect any differences in H2A.Z enrichment between 24 and 72 hours of DMSO treatment. This indicates that any compensatory effect caused by Srcap knockdown does not influence overall H2A.Z levels into chromatin (Supplementary Figure 4). Next, we analyzed the RA-treated data to determine whether RA treatment affects H2A.Z levels. Notably, both H2A.Z-regulated genes and developmental genes displayed H2A.Z enrichment at 72 hours compared to 24 hours in shScr controls (Fig. 10B). This suggests that H2A.Z accumulates in response to developmental stimuli following its initial decrease. Remarkably, sh*Srcap* cells did not display a significant enrichment of H2A.Z at 72 hours at *Fos, Arc, Nr4a2* and *Sox5*, indicating that Srcap plays a role in mediating H2A.Z incorporation following developmental stimuli (Fig. 10B). Notably, *Egr1* showed increased H2A.Z enrichment at 72h in sh*Srcap*-treated cells; however, this increase is significantly lower relative to shScr controls (Fig. 10B). In contrast, *Fezf2* is indistinguishable from shScr controls, indicating the presence of alternative mechanisms for H2A.Z incorporation (Fig. 10B). Overall, these findings demonstrate that Srcap is critical for H2A.Z re-incorporation during neuronal differentiation, underscoring its role in neurodevelopmental chromatin dynamics.

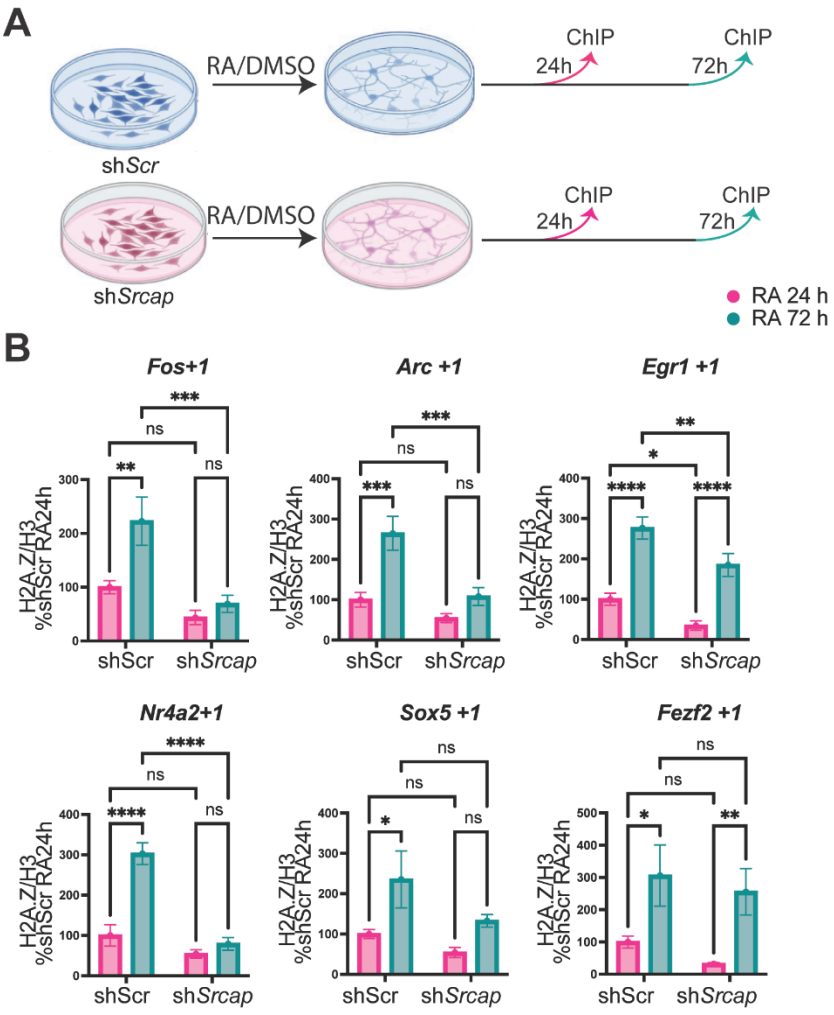

Figure 10: Knockdown of Srcap prevents incorporation of H2A.Z during differentiation. **(A)** Schematic representation of experimental workflow in cultured N2A cells. **(B)** ChIP data in Figure 9 were re-analyzed to compared H2A.Z occupancy at the +1 nucleosome between 24 hours (n = 6) and 72 hours (n = 6) into differentiation with RA. H2A.Z abundance is normalized to H3, and data are expressed as % compared to shScr RA 24h. Data are expressed as mean ± SEM. Two-way ANOVA *p < 0.05.

2.4.4 Developmental-induced gene expression is altered in the absence of *Srcap.*

Activity-dependent removal of H2A.Z has been linked to gene expression changes, particularly in hippocampus-related genes[5,21]. Similarly, the loss of H2A.Z-removing chaperone Anp32e alters gene expression during activity-dependent processes[6]. However, little is known about how H2A.Z dynamics affect developmental gene expression. To investigate whether Srcap activity on H2A.Z directly regulates neurodevelopmental gene expression, we knocked down *Srcap* in N2A cells and treated them with RA for 24 and 72 hours (Fig. 11A). We then measured the expression levels of

H2A.Z target and neurodevelopmental genes. All the tested genes showed altered expression dynamics in *Srcap*-knockdown cells compared to controls (Fig. 11B-C). Specifically, in shScr control cells, *Fos* and *Arc,* showed an increase and decrease, respectively, while *Egr1* displayed no change at both 24 and 72h of RA (Fig. 11B-C). However, *Srcap* knockdown disrupted these dynamics, such that *Fos* failed to display any developmental-induced increase at 24 and 72 h of RA treatment (Fig. 11B-C). In contrast, *Arc* did not recapitulate developmental-induced reduction upon depletion of Srcap at 24h of RA (Fig. 11B). Still, its expression was indistinguishable from shScr control at 72h (Fig. 11C), suggesting a delayed response in *Srcap*-depleted cells. Finally, *Egr1* expression was reduced as an effect of development at 24 and 72h (Fig. 11B-C).

Nr4a2, a gene associated with neurodevelopment, showed increased expression at 24 and 72 h of RA treatment in shScr cells, while *Sox5* and *Fezf2* exhibited increased expression at only 72h (Fig. 11B-C). Upon *Srcap* depletion, *Nr4a2* did not display an increase in expression at 24h (Fig. 11B). Still, it demonstrated significant developmentally induced expression at 72h of RA treatment (Fig. 11C), suggesting a delay in induction in *Srcap*-depleted cells, similar to *Arc*. In addition, *Sox5* expression was not induced at 72h of RA treatment in sh*Srcap* cells (Fig. 11C). Finally, there was a significant increase in *Fezf2* expression at 24h of RA treatment in sh*Srcap* cells (Fig. 11B), relative to shScr controls.

These results demonstrate that the absence of Srcap disrupts developmental gene expression, primarily through altered timing or complete loss of induction, highlighting Srcap's key role in regulating neurodevelopmental transcriptional programs.

The steady-state expression of most candidate genes is altered by the knockdown of Srcap. Specifically, *Arc, Sox5* and *Fezf2* show reduced expression, while *Egr1* and *Nr4a2* are upregulated exclusively in response to Srcap knockdown (Fig. 11B, grey bars). However, these effects are

abolished or reversed by 72h, with *Arc, Sox5, Nr4a2* and *Fezf2* showing no significant differences between shScr and shSrcap, while *Fos* exhibits enhanced expression. Egr1 expression remains increased as an effect of the knockdown (Fig. 11C, grey bars). These time-dependent changes suggest that Srcap knockdown does not permanently impair gene expression but rather delays or dysregulates the typical transcriptional trajectory. In addition, the recovery of many genes at 72 h suggests that cells may undergo compensatory mechanisms over time to partially restore gene expression despite the absence of *Srcap* as observed in Supplementary Figure S3.

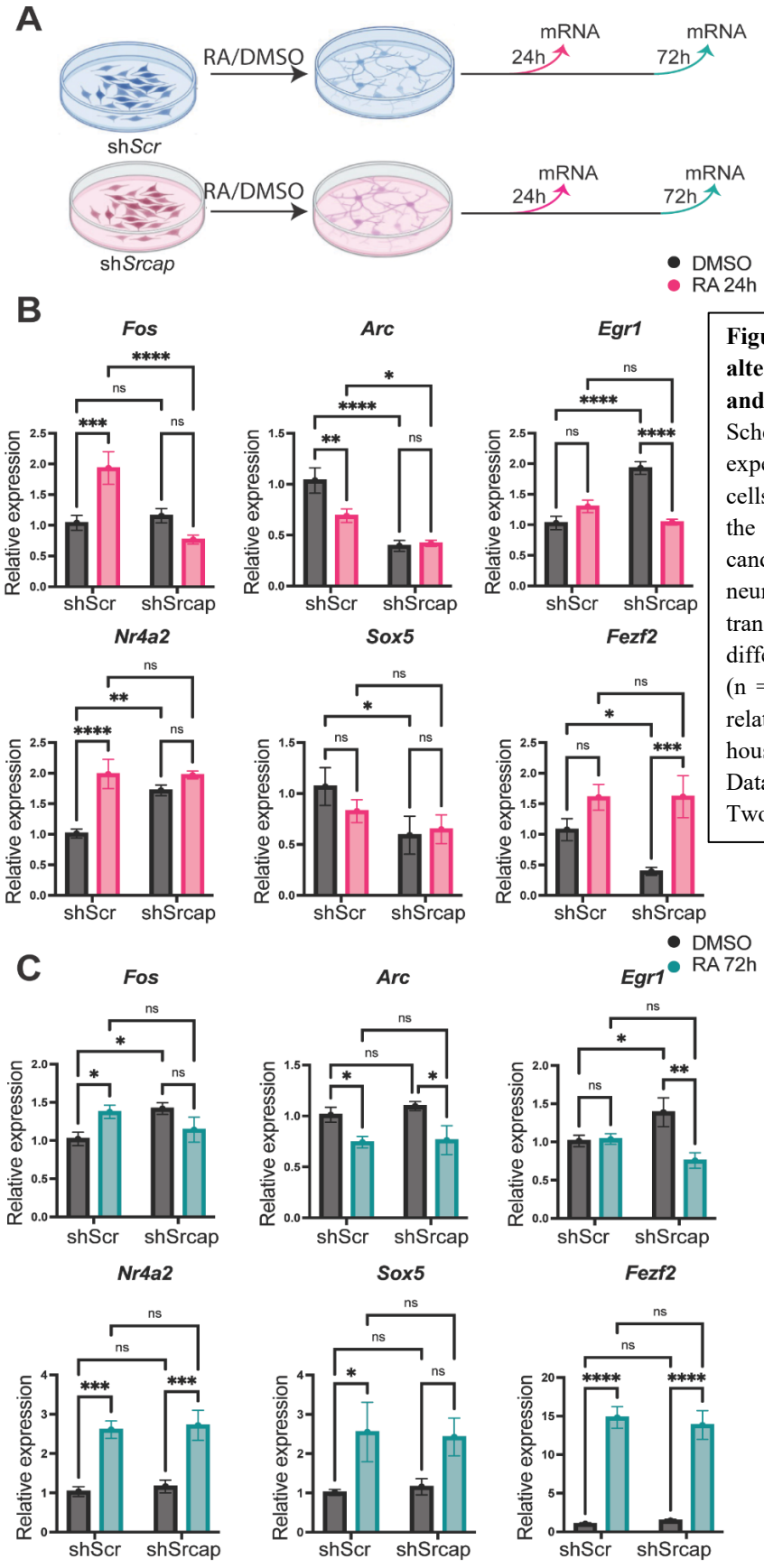

Figure 11: Knockdown of Srcap alters gene expression of neuronal and developmental genes. (A) Schematic representation of experimental workflow in cultural N2A cells. **(B-C)** qPCR was used to measure the change in gene expression for candidate activity-dependent and neurodevelopmental genes in N2A cells transfected with shSrcap and differentiated with RA for **(B)** 24 hours (n = 6) or **(C)** 72 hours (n = 6). The relative expression was normalized to housekeeping genes Gapdh and ActB. Data are expressed as mean ± SEM. Two-way ANOVA *p < 0.05.

2.5 Discussion

Our study reveals the critical role of Srcap in regulating H2A.Z dynamics and gene expression during neuronal differentiation, highlighting its importance in neurodevelopment. By demonstrating that Srcap deficiency disrupts H2A.Z occupancy, its abundance following neurodevelopmental stimuli, and the temporal regulation of neurodevelopmental genes, we provide new insights into how Srcap influences transcriptional programs required for proper neuronal differentiation.

2.5.1 Srcap, H2A.Z, and CBP

Our findings are consistent with prior research demonstrating that Srcap is essential for H2A.Z incorporation into chromatin[14,19,20]. Here, we show that Srcap-mediated H2A.Z deposition occurs not only at activity-dependent genes, such as *Fos, Arc,* and *Egr1*, but also at neurodevelopmental genes, including *Sox5, Nr4a2*, and *Fezf2* (Fig. 7). Interestingly, our findings show that Srcap loss does not impair the recruitment of the histone acetyltransferase CBP to these genes, nor does it affect global levels of H3 acetylation, the downstream target of CBP (Fig. 8). These results are consistent with previous work demonstrating that a Srcap isoform lacking the CBP-binding domain activates transcription *in vitro* at levels comparable to those of full-length Srcap[25]. We speculate that Srcap primarily regulates transcription by influencing H2A.Z dynamics. However, we cannot exclude the possibility that CBP recruitment may serve as a secondary function or may operate at loci and genomic regions not tested in this study.

2.5.2 Srcap mediates H2A.Z dynamics during development and differentiation

Previous data link Srcap to H2A.Z incorporation and Anp32e to H2A.Z removal[26]. Interestingly, our data show that Srcap loss impairs developmental-dependent H2A.Z removal (Fig. 9), something we and others previously linked to Anp32e loss[6,27–30]. Notably, low genomic levels of H2A.Z have been observed at early developmental stages and shown to prevent early differentiation[28]. It is possible that, after a developmental stimulus, H2A.Z is removed to promote chromatin plasticity before the establishment of fully differentiated chromatin states. The lack of H2A.Z removal in Srcap-depleted cells may result from the already low levels of H2A.Z. We speculate that global levels of H2A.Z can influence its dynamics independently of its chaperones, whereby low chromatin H2A.Z presence may limit further removal through a feedback mechanism that influences Anp32e activity. We propose that protein levels of H2A.Z chaperones Srcap and Anp32e regulate chromatin levels of H2A.Z as much as chromatin levels of H2A.Z regulate the activity of its chaperones.

In addition to this, H2A.Z dynamics are also influenced by RNA Polymerase II activity. Specifically, in the yeast *S. Cerevisiae*, *HTZ1* (the H2A.Z homolog) is enriched at promoters and is displaced as Pol II progresses[31], facilitating transcription initiation and elongation. Similarly, H2A.Z is associated with Pol II pausing in *Drosophila* and is removed upon gene activation[32]. This suggests transcriptional activity may also mediate H2A.Z removal upon N2A RA-mediated differentiation. However, direct evidence of Pol II-mediated eviction of H2A.Z is lacking in mammalian systems. Studies in mouse brain and primary neurons have shown that while transcription of immediate early genes is induced within minutes, H2A.Z removal from their promoters occurs much later, suggesting that Pol II is not the primary driver of H2A.Z eviction[5,21].

The same studies also demonstrated that H2A.Z removal in the hippocampus following a stimulus is correlated with increased gene expression at later stages[5], further highlighting the complex relation between H2A.Z dynamics and transcription.

Our data also highlight distinct chromatin adaptations in response to RA treatment and Srcap knockdown. Specifically, we show that H3 levels increase 24 hours following RA treatment (Supplementary Figure 3), suggesting that differentiation-induced genome reorganization occurs independently of Srcap. While we did not observe any change in H3 occupancy after 48h transfection with sh*Srcap* (Supplementary Figure 1), we did observe a significant increase in nucleosome number after 96 hours (Supplementary Figure 3C). This indicates that adaptive mechanisms happen in cells following Srcap knock down in a time-dependent manner.

Our studies also highlight a more nuanced role for Srcap in mediating H2A.Z re-incorporation during retinoic acid (RA)-induced differentiation (Fig. 10). This is the first study observing the effects of loss of Srcap on H2A.Z across different developmental time-points and suggests that Srcap is necessary to ensure proper H2A.Z incorporation across neurodevelopment and possibly establish stable chromatin states. Notably, we observed that genes like *Fezf2* and *Egr1* retained some H2A.Z dynamics even in the absence of Srcap, suggesting that additional pathways may compensate for Srcap loss in a gene-specific manner. Particularly, remodelers p400 and NuRD have been identified to play a role in H2A.Z incorporation[7,33], indicating that Srcap role may be gene specific.

2.5.3 Loss of Srcap influences the timing of developmental gene expression

Our gene expression results highlight Srcap's pivotal role in regulating genes' dynamics during neuronal differentiation (Fig. 11). We observed profound disruptions in the temporal dynamics

and induction of crucial genes, shedding light on how chromatin remodelling by Srcap influences transcriptional programs.

The observed disruptions in *Fos, Arc,* and *Egr1* expression align with prior studies implicating H2A.Z dynamics in regulating activity-dependent gene expression during memory formation[5,6,21]. However, our findings reveal a previously uncharacterized role for Srcap in coordinating these dynamics during developmental processes. Specifically, the failure of *Fos* induction and delayed repression of *Arc* highlight Srcap's importance in ensuring precise temporal control of gene expression, consistent with its role in H2A.Z deposition. We also show that Srcap regulates genes critical for neuronal differentiation and brain development. The delayed induction of *Nr4a2* and failure to induce *Sox5* suggest that Srcap-mediated chromatin remodelling is essential for timely gene activation. The aberrant early expression of *Fezf2* further suggests that Srcap loss leads to dysregulated transcriptional timing, potentially disrupting developmental pathways. Notably, we could not identify a reliable gene expression alteration pattern, aligning with the dual roles of H2A.Z in gene expression regulation[34]. Our previous studies regarding the role of H2A.Z and its chaperones in activity-dependent gene expression also failed to identify clear directions of gene expression alterations[5,6], indicating that the regulation of H2A.Z dynamics can have diverse and profound effects on gene expression.

We also observed disrupted steady-state gene expression upon Srcap loss at 24h, with many genes recovering their expression by 72h. This recovery suggests that alternative regulatory pathways may compensate for *Srcap* loss, potentially through chromatin remodeling factors with overlapping functions, as indicated by the increased nucleosome occupancy observed at 96 h after transfection (Supplementary Figure 3C). However, the inability of cells to fully compensate for

Srcap loss highlights its critical role in maintaining proper differentiation and gene expression balance over time.

2.5.4 Limitations

One limitation of our study is the use of N2A cells as a model for neuronal differentiation. While these cells provide a convenient system to study neurodevelopmental processes, they lack the complexity of primary neurons or *in vivo* systems. Thus, our findings may not fully capture the interplay between Srcap, H2A.Z, and transcriptional regulation in more physiologically relevant contexts. Future studies using primary neurons, brain organoids, or *in vivo* models are necessary to validate and extend our results.

Another limitation is the focus on a select set of genes. While our findings highlight Srcap's role in regulating H2A.Z dynamics and gene expression at specific loci, it remains unclear whether these effects are representative of genome-wide patterns. High-throughput analyses such as CUT&Tag and scRNA-seq could provide a more comprehensive view of Srcap's impact on chromatin remodelling and gene expression.

2.5.5 Conclusions

This work establishes Srcap as a critical regulator of developmental H2A.Z dynamics, linking its activity to neurodevelopmental gene expression. Furthermore, we demonstrate that Srcap mediates not only H2A.Z deposition but also its developmental-induced re-incorporation, revealing a previously uncharacterized role for this chromatin remodeler in resetting chromatin states during differentiation.

Based on our findings, we speculate that SRCAP acts as a chromatin "reset button." By maintaining H2A.Z chromatin levels, Srcap facilitates the removal of H2A.Z during early

developmental signals. Subsequently, Srcap enables H2A.Z re-incorporation to establish stable chromatin states. This dynamic regulation likely ensures that neurodevelopmental genes are activated at the right time and place, preventing premature or delayed differentiation. Notably, SRCAP mutations are linked to the development of various neurodevelopmental disorders (NDDs)[35–38]. Therefore, dysregulation of Srcap-mediated H2A.Z dynamics may contribute to the etiology of SRCAP-related disorders by disrupting the temporal regulation of gene expression critical for brain development.

In conclusion, our study underscores the importance of SRCAP in orchestrating H2A.Z dynamics and neurodevelopmental gene expression, offering new insights into its role as a chromatin remodeler. By bridging the gap between chromatin biology and neuronal differentiation, these findings provide a foundation for future research into the molecular underpinnings of neurodevelopmental disorders and potential therapeutic strategies.

2.6 Acknowledgements

This research was supported by an NSERC Discovery Grant, NSERC Discovery Accelerator Supplement to GS.

2.7 Author Contributions

K.S.J. and G.S. designed the project and co-wrote the manuscript. K.S.J., S.A.Y., S.M.I., L.A.D-M., and I.R.G. performed the experiments.

2.8 Data Availability

Data generated during this study are available from the corresponding author upon reasonable request.

2.9 Declaration of interests

The authors declare no competing interests.

2.10 References

1. María J Barrero, Stephanie Boué, & Juan Carlos Izpisúa Belmonte. Epigenetic mechanisms that regulate cell identity. *Cell Stem Cell* **7**, 565–70 (2010).
2. Steven Henikoff & M Mitchell Smith. Histone Variants and Epigenetics. *Cold Spring Harb Perspect Med.* **7**, 1 (2015).
3. Mylène Brunelle *et al.* The histone variant H2A.Z is an important regulator of enhancer activity. *Nucleic Acids Res* **43**, 9742–56 (2015).
4. Benedetto Daniele Giaimo, Francesca Ferrante, Andreas Herchenröther, Sandra B Hake, & Tilman Borggrefe. The histone variant H2A.Z in gene regulation. *Epigenetics Chromatin* **12**, 37 (2019).
5. Stefanelli, G. *et al.* Learning and Age-Related Changes in Genome-wide H2A.Z Binding in the Mouse Hippocampus. *Cell Rep* **22**, 1124–1131 (2018).
6. Stefanelli, G. *et al.* The histone chaperone Anp32e regulates memory formation, transcription, and dendritic morphology by regulating steady-state H2A.Z binding in neurons. *Cell Rep* **36**, 109551 (2021).
7. Michael S Kobor *et al.* A protein complex containing the conserved Swi2/Snf2-related ATPase Swr1p deposits histone variant H2A.Z into euchromatin. *PLoS Biol* **2**, E131 (2004).
8. Xiaoping Liang *et al.* Structural basis of H2A.Z recognition by SRCAP chromatin-remodeling subunit YL1. *Nat Struct Mol Biol* **23**, 317–23 (2016).
9. Ruhl, D. *et al.* Purification of a human SRCAP complex that remodels chromatin by incorporating the histone variant H2A.Z into nucleosomes. *Biochemistry* **45**, 5671–7 (2006).
10. Madeline M Wong, Linda K Cox, & John C Chrivia. The chromatin remodeling protein, SRCAP, is critical for deposition of the histone variant H2A.Z at promoters. *J Biol Chem* **282**, 26132–9 (2007).
11. Chih-Chao Hsu *et al.* Gas41 links histone acetylation to H2A.Z deposition and maintenance of embryonic stem cell identity. *Cell Discov* **4**, (2018).

12. Ye, B. *et al.* The chromatin remodeler SRCAP promotes self-renewal of intestinal stem cells. *EMBO J* **39**, e103786 (2020).

13. Yang Yang *et al.* HIRA complex presets transcriptional potential through coordinating depositions of the histone variants H3.3 and H2A.Z on the poised genes in mESCs. *Nucleic Acids Res* **50**, 191–206 (2022).

14. Ana Cuadrado *et al.* Essential role of p18Hamlet/SRCAP-mediated histone H2A.Z chromatin incorporation in muscle differentiation. *EMBO J* **29**, 2014–25 (2010).

15. Mingjie Xu *et al.* The SRCAP chromatin remodeling complex promotes oxidative metabolism during prenatal heart development. *Development* **148**, dev199026 (2021).

16. Chun-Wei Chen *et al.* SRCAP mutations drive clonal hematopoiesis through epigenetic and DNA repair dysregulation. *Cell Stem Cell* **30**, 1503–19 (2023).

17. Ye, B. *et al.* Suppression of SRCAP chromatin remodelling complex and restriction of lymphoid lineage commitment by Pcid2. *Nat Commun* **8**, 1518 (2017).

18. H Johnston, J Kneer, I Chackalaparampil, P Yaciuk, & J Chrivia. Identification of a novel SNF2/SWI2 protein family member, SRCAP, which interacts with CREB-binding protein. *J Biol Chem* **274**, 16370–16376 (1999).

19. Rachel S Greenberg, Hannah K Long, Tomek Swigut, & Joanna Wysocka. Single Amino Acid Change Underlies Distinct Roles of H2A.Z Subtypes in Human Syndrome. *Cell* **178**, 1421–36.e24 (2019).

20. Armelle Tollenaere *et al.* Mechanisms of gene regulation by SRCAP and H2A.Z. *Nat Commun* **17**, 3560 (2026).

21. Iva B Zovkic, Brynna S Paulukaitis, Jeremy J Day, & J David Sweatt. Histone H2A.Z subunit exchange controls consolidation of recent and remote memory. *Nature* **515**, 582–6 (2014).

22. Michal Lipinski, Beatriz Del Blanco, & Angel Barco. CBP/p300 in brain development and plasticity: disentangling the KAT's cradle. *Curr Opin Neurobiol* **59**, 1–8 (2019).

23. Ryan A Henry, Yin-Ming Kuo, & Andrew J Andrews. Differences in specificity and selectivity between CBP and p300 acetylation of histone H3 and H3/H4. *Biochemistry* **52**, (2013).

24. Brian T Weinert *et al.* Time-Resolved Analysis Reveals Rapid Dynamics and Broad Scope of the CBP/p300 Acetylome. *Cell* **174**, 231-244.e12 (2018).

25. M A Monroy *et al.* Regulation of cAMP-responsive element-binding protein-mediated transcription by the SNF2/SWI-related protein, SRCAP. *J Biol Chem* **276**, 40721–40726 (2001).

26. Karanveer S Johal, Manjinder S Cheema, & Gilda Stefanelli. Histone Variants and Their Chaperones: An Emerging Epigenetic Mechanism in Neurodevelopment and Neurodevelopmental Disorders. *J Integr Neurosci* **22**, 108 (2023).

27. Ozge Gursoy-Yuzugullu, Marina K Ayrapetov, & Brendan D Price. Histone chaperone Anp32e removes H2A.Z from DNA double-strand breaks and promotes nucleosome reorganization and DNA repair. *Proc Natl Acad Sci U S A* **112**, 7507–12 (2015).

28. Fabian N Halblander, Fanju W Meng, & Patrick J Murphy. Anp32e protects against accumulation of H2A.Z at Sox motif containing promoters during zebrafish gastrulation. *Dev Biol* **507**, 34–43 (2024).

29. Obri, A. *et al.* ANP32E is a histone chaperone that removes H2A.Z from chromatin. *Nature* **505**, 648–53 (2014).

30. Kristin E Murphy, Fanju W Meng, Claire E Makowski, & Patrick J Murphy. Genome-wide chromatin accessibility is restricted by ANP32E. *Nat Commun* **11**, 5063 (2020).

31. Anand Ranjan *et al.* Live-cell single particle imaging reveals the role of RNA polymerase II in histone H2A.Z eviction. *Elife* **9**, e55667 (2020).

32. Constantine Mylonas, Choongman Lee, Alexander L Auld, Ibrahim I Cisse, & Laurie A Boyer. A dual role for H2A.Z.1 in modulating the dynamics of RNA polymerase II initiation and elongation. *Nat Struct Mol Biol* **28**, 435–442 (2021).

33. Yue Yang *et al.* Chromatin remodeling inactivates activity genes and regulates neural coding. *Science* **353**, 300–305 (2016).

34. Maud Marques, Liette Laflamme, Alain L Gervais, & Luc Gaudreau. Reconciling the positive and negative roles of histone H2A.Z in gene transcription. *Epigenetics* **5**, 267–72 (2010).

35. Ivan Iossifov *et al.* The contribution of de novo coding mutations to autism spectrum disorder. *Nature* **515**, 216–221 (2014).

36. Ivan Iossifov *et al.* De novo gene disruptions in children on the autistic spectrum. *Neuron* **74**, 285–99 (2012).

37. Rebecca L Hood *et al.* Mutations in SRCAP, encoding SNF2-related CREBBP activator protein, cause Floating-Harbor syndrome. *Am J Hum Genet* **90**, 308–13 (2012).

38. Rots, D. *et al.* Truncating SRCAP variants outside the Floating-Harbor syndrome locus cause a distinct neurodevelopmental disorder with a specific DNA methylation signature. *Am J Hum Genet* **108**, 1053–1068 (2021).

Chapter 3: Role of Srcap in Cortical Development and Behavioural Regulation

3.1 Abstract

Neurodevelopment relies on the precise regulation of gene expression to coordinate the generation, differentiation, and organization of neurons. Epigenetic regulators and chromatin remodelers play central roles in these processes, and their disruption contributes to the etiology of NDDs. Among these, SRCAP is a large chromatin remodelling complex responsible for exchanging the canonical histone H2A with its variant, H2A.Z, which plays important regulatory roles in early development and neurodevelopment. Despite strong genetic links between SRCAP dysfunction and NDDs, its roles and functions in neurodevelopment as well as the molecular mechanisms underlying SRCAP-related diseases remain unknown. Here, we investigated the role of Srcap in neurodevelopment by assessing cortical and ventricular structures, neural progenitor populations, and adult behaviour associated with NDDs using a cortex-specific conditional Srcap knockout mouse model. Immunofluorescence of embryonic coronal brain slices revealed reductions in cortical thickness, ventricular area, and cortical area implicating Srcap as an important regulator of progenitor proliferation and neuronal differentiation. In addition, behaviour analysis of adult mice with loss of one *Srcap* allele (cHet) revealed alterations in anxiety-related and exploratory behaviours. Together, these findings show that Srcap has a critical role in neurodevelopment and that loss of Srcap disrupts cortical development and adult behaviours.

Keywords: histone variant, histone chaperone, H2A.Z, Srcap, cortical development, behaviour

3.2 Introduction

While N2A cells provide a simple model by which we can study H2A.Z occupation and gene expression dynamics, they lack the complex multi-faceted signaling environment that is observed in *in vivo* brain development. As such, they can only provide limited insight into neurodevelopmental processes. On the contrary, *in vivo* models enable the investigation of neurodevelopment within the context of intact tissue architecture, cellular interactions, and developmental signaling pathways that collectively shape brain development.

Rodents have commonly been used as a model in neuroscience because they share molecular and cellular processes in cortical development with humans[1]. Cortical development follows a broadly genetically conserved program in both humans and mice with a notable difference being developmental timing. As such, transgenic mouse models have historically been used to investigate genes implicated in neurodevelopment and in NDDs to investigate their functions[2]. As far as the investigation of Srcap and its involvement in H2A.Z dynamics is concerned, these proteins are highly conserved in humans and mice, which motivated us to use a mouse model for this study. Together, these findings support the use of mouse models to study SRCAP function during cortical development and provide a strong rationale for investigating SRCAP-mediated chromatin remodelling mechanisms in the developing mouse brain.

Considering *Srcap* null mice are not viable[3], we decided to generate a new conditional knockout mouse model in which *Srcap* is ablated in the developing cortex. We then assessed if the loss of Srcap affected four key morphological characteristics of the mice cortices, total cortical area, cortical thickness, total cell count, and total ventricular area. In addition, to determine if there are disruptions in laminar organization, we looked at patterns of cortical layer markers. The

behavioural characterization involved measuring changes in anxiety, memory, and sociability as these are behaviours that are commonly associated with NDDs.

We observed that loss of Srcap caused significant abnormalities in the structures of the mice brains, altering total cortical area, cortical thickness, cell number, and ventricular zone area. Disruptions were also seen in laminar zone organization with a reduction in neural progenitor populations in both the VZ and the SVZ. The behavioural characterization revealed changes in anxiety-like and exploratory behaviours in mice missing one allele of *Srcap*, but no change in memory or sociability. Overall, these results suggest that loss of Srcap contributes to impaired cortical development and that the impairments are accompanied by behaviour defects.

3.3 Materials and Methods

3.3.1 Animal Husbandry

All animal procedures were approved by the University of Ottawa Animal Care and Veterinary Service (ACVS) and conducted in accordance with the guidelines of the Canadian Council on Animal Care (CCAC). Mice were housed in a temperature- and humidity-controlled facility under a 12 h light-dark cycle with ad libitum access to food and water. Animals were monitored daily to ensure welfare and all efforts were made to minimize animal discomfort and distress throughout the study.

3.3.2 Mouse Model

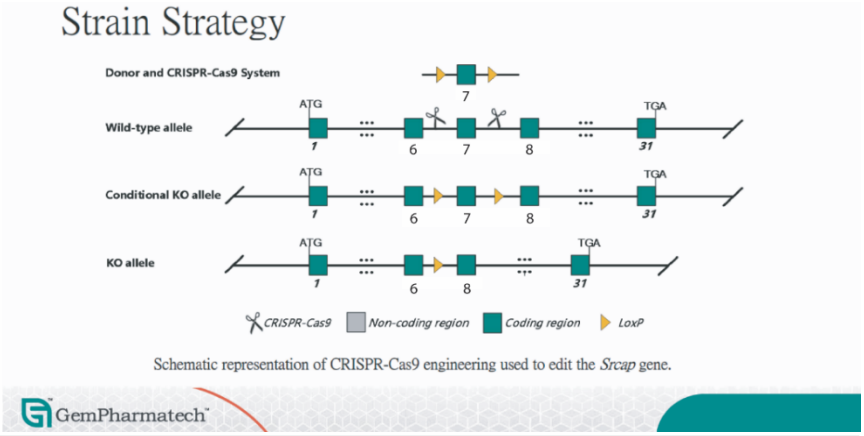

Figure 12: Srcap conditional knock-out strategy. LoxP sites have been inserted around exon 7. Cre excision will result in a frameshift and premature stop.

GemPharmatech generated *Srcap*$^{fl/+}$ mice using CRISPR-Cas9, to introduce LoxP sites flanking exon 7 of one allele of *Srcap.* Cre recombination leads to the excision of exon 7, producing a frameshift mutation and a premature stop codon at amino acid 301[4] (Fig. 12).

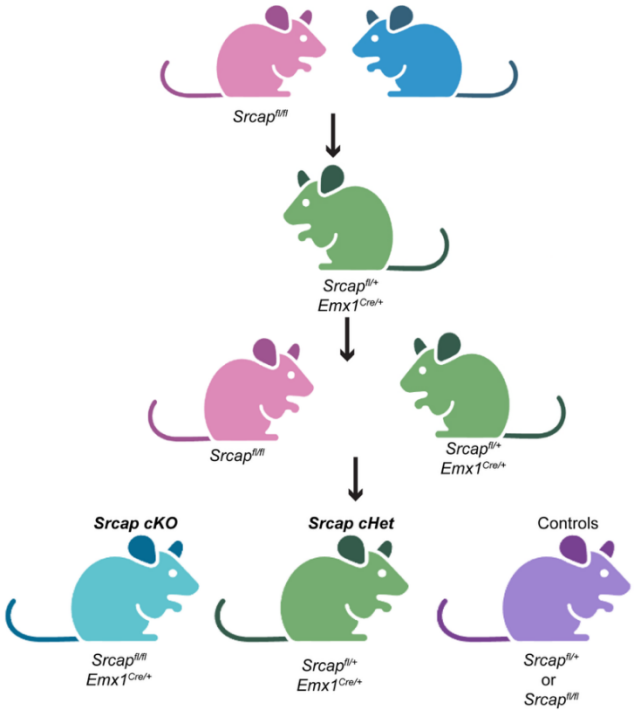

Figure 13: Transgenic mice breeding scheme and experimental groups.

To generate conditional knockouts and heterozygous animals, *Srcap*$^{fl/+}$ mice were crossed with *Srcap*$^{fl/+}$ mice to produce *Srcap*$^{fl/fl}$ mice (Fig. 13). *Srcap*$^{fl/fl}$ mice were crossed with *Emx1*^{cre} mice (Jax, strain #005628), expressing Cre recombinase from the *Emx1* locus. This locus is active in NPCs in the neocortex beginning at E10.5, which marks the start of neurogenesis in mice[5]. The *Srcap*$^{fl/+}$ *Emx1*$^{cre/+}$ mice were bred with *Srcap*$^{fl/fl}$ mice to produce the experimental groups (Fig. 13). *Srcap*$^{fl/fl}$ *Emx1* ^{Cre} (***Srcap* cKO)** and *Srcap*$^{fl/+}$ *Emx1* ^{Cre} **(*Srcap* cHet)** were used as separate experimental groups. *Srcap*$^{fl/fl}$ and

Srcap$^{fl/+}$ mice served as controls. All experimental groups were compared to controls and to each other to assess the impact of losing one or two *Srcap* alleles. As sex-related components affect brain development and H2A.Z dynamics display sex differences[6], all research involved both female and male animals

3.3.3 Genotyping

The genotyping strategy used for the Srcap mouse line was provided by GemPharmatech (Fig. 14A). It entails one primer within exon 7 of *Srcap* and one in the adjacent intronic region. The LoxP insertion between these primers increases the PCR amplicon size by ~106 bp. Two sets of primers were given, each targeting different sides of exon 7; however, the 3' arm primers produced sharper bands that are more easily distinguishable and were primarily used to conduct genotyping. In WT mice, the 3' arm primers produced a band of 290 base pairs (bp), and in the *Srcap*$^{fl/fl}$ mice, the primers produced a band of 396 bp (Fig. 14B).

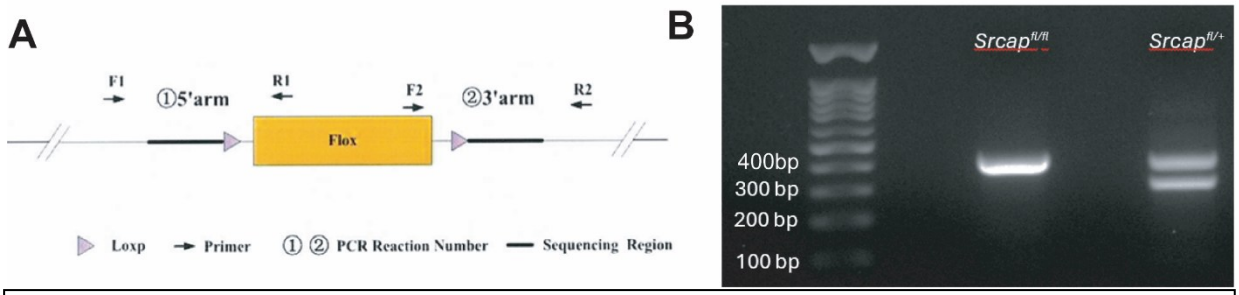

Figure 14: Genotyping strategy. (A) Primer design. **(B)** PCR using 3'arm primer pair produces a 396-bp product from the floxed Srcap allele (Srcap$^{fl/fl}$) and a 290-bp product from the WT allele (Srcap$^{+/+}$). The larger band corresponds to the presence of the LoxP insertion.

The embryonic tissue was submerged in 100 µl of alkaline lysis buffer (pH 12, 25 mmol/L NaOH, 0.2 mmol/L EDTA) and incubated at 95 °C for 30 minutes, followed by 10 minutes at 4 °C. 100 µl of neutralization buffer (pH 5, 40 mmol/L Tris) was added. To a new tube, 100 µl of DNA was mixed with 100 µl of Phenol:Chloroform:Isoamylic alcohol (Invitrogen, 15593031). Samples were centrifuged at 17,000xG for 10 minutes. The aqueous layer was transferred to a separate tube

containing 5 µl of 3 mol/L NaAc (pH 5.2) and vortexed. 137.5 µl of ice-cold 95% EtOH was added, and the mixture was vortexed and incubated overnight at -20°C. Samples were centrifuged at 17,000xG for 30 minutes at 4°C, and the supernatant was decanted. 150 µl of ice cold 75% EtOH was added, and the sample was centrifuged at 17,000xG for 10 minutes at 4°C. The supernatant was decanted, and the pellet was air-dried and resuspended in 20 µl of ultrapure water, then diluted 1:10 for PCR.

Adult tissues were processed like embryonic tissues, skipping the phenol/chloroform purification. A PCR master mix was made according to Table 3 for Srcap genotyping, Table 4 for Exm1 genotyping (make two separate mastermixes, each with a unique reverse primer and combine the samples after the PCR), and Table 5 for sex genotyping. The mastermix was added to the PCR tubes, along with the DNA (4 µl for Srcap and sex, and 0.5 µl for Emx1). For each PCR, a blank and an heterozygous control were added. The samples were run in a thermocycler with the PCR Protocol for Srcap (Table 6), Emx1 (Table 7), or sex (Table 8). Samples were loaded on a 1.5% TAE/Agarose gel and run at 80-100V for 40-50 minutes. The sequences for the genotyping primer are listed in Table 9.

Table 3: Srcap genotyping mastermix formula

Reagent	Volume Per Sample (µl)
GoTaq Polymerase	12.5
Forward Primer	1
Reverse Primer	1
ddH_2O	6.5

Table 4: Emx1 genotyping mastermix formula

Reagent	Volume Per Sample (µl)
GoTaq Polymerase	5
Forward Primer	1
Reverse Primer	1
ddH_2O	2.5

Table 5: Sex genotyping mastermix formula

Reagent	Volume Per Sample (µl)
GoTaq Polymerase	10
Forward Primer	1
Reverse Primer	1
ddH_2O	4

Table 6: Srcap PCR Protocol

Step	Temperature (ºC)	Time	Cycles
1	95	5 minutes	1X
2	98	30 seconds	20X (-0.5ºC/Cycle)
3	65	30 seconds	
4	72	45 seconds	
5	98	30 seconds	20X
6	55	30 seconds	
7	72	45 seconds	
8	72	5 minutes	1X
9	10	Hold	

Table 7: Emx1 PCR Protocol

Step	Temperature (ºC)	Time	Cycles
1	95	3 minutes	1X
2	95	15 seconds	10X (-0.6ºC/Cycle)
3	68	15 seconds	
4	72	30 seconds	
5	95	15 seconds	20X
6	62	15 seconds	
7	72	30 seconds	
8	72	5 minutes	1X
9	12	Hold	

Table 8: Sex PCR Protocol

Step	Temperature (°C)	Time	Cycles
1	94	2 minutes	1X
2	94	30 seconds	35X
3	57	30 seconds	
4	72	30 seconds	
5	72	5 minutes	1X
6	10	Hold	

Table 9: Primers used for Genotyping

Primer Name	Primer Sequence
Sex Forward	GATGATTTGAGTGGAAATGTGAGGTA
Sex Reverse	CTTATGTTTATAGGCATGCACCATGTA
Srcap 3' arm Forward	GGTTTCTCGACTGGATGATGAAGG
Srcap 3' arm Reverse	GAGCAGCTCTTCCAGTGGCAGTT
Cre Forward	CAACGGGGAGGACATTGA
Cre WT Reverse	CAAAGACAGAGACATGGAGAGC
Cre Mut Reverse	TCGATAAGCCAGGGGTTC

3.3.4 Western blotting

Transfected cells were washed with PBS (GIBCO, 14190-136) and scraped into 200 µl of 6X sample buffer (176 µl loading dye [6.6 ml 0.5M Tris pH 6.8, 3.4 ml glycerol, 1 g SDS, 0.1 g Bromophenol blue], 24 µl B-2 Mercaptoethanol [BioShop MER002]) per well. Samples were then boiled at 95℃ for 5 min, and 25 µl were loaded on the gel with 5 µl of protein ladder (Bio-Rad,1610374). Proteins were separated on a 15% gel using SDS-PAGE. The gel box was filled with run buffer (1X Tris Glycine/SDS Buffer, BioRad 1610772) and then transferred for 1h at 0.4 amps to a PVDF membrane (Millipore, IPVH00010). The transfer box was filled with a transfer buffer (200 ml MeOH; 100 mL 10X Tris/Glycine Buffer, BioRad 1610771; 700 ml distilled water). Membranes were blocked in TBS-T containing 5% milk for 1hr at RT and then incubated with primary antibodies: pH3 (acetyl K9, K14, K18, K23, K27, abcam AB47915, 1:1000, overnight) and Tubulin (NEB 15115S, 1:10.000, 1 h). After washing, membranes were incubated with appropriate secondary antibody (Life Technologies, 12005869, 1:1000) for 1 h at RT. Detection was performed using a BioRad ChemiDoc, and image analysis was conducted with Fiji/Imagej (NIH).

Adult cortices were lysed in RIPA buffer and dounce homogenized with 10 strokes. The lysate was incubated 10 min on ice followed by centrifugation at 13,000 rpm 4 ºC. The Pierce BCA Protein Assay Kit (ThermoScientific, 23227) was used to determine protein concentrations.

After adding loading dye, samples were heated at 70°C for 10 min and run on a 4-20% gradient gel and then transferred for 1.5h at 100V to a PVDF membrane (Millipore, IPVH00010). Membranes were blocked in TBS-T containing 5% milk for 1hr at RT and then incubated with primary antibodies: Srcap (Bioss BS-12119R1:500, overnight) and Tubulin (NEB 15115S, 1:10.000, 1 h). After washing, membranes were incubated with appropriate secondary antibody (Life Technologies, 12005869, 1:500) for 1 h at RT. Detection was performed using a BioRad ChemiDoc, and image analysis was conducted with Fiji/Imagej (NIH).

3.3.5 Cryosectioning of embryonic brains

Brains from E15 mouse embryos were dissected and submerged in 4% Paraformaldehyde (Electron Microscopy Sciences 15710)/PBS overnight at 4°C. The brains were transferred to 20% sucrose/PBS (weight/volume) solution and stored at 4°C overnight and then transferred to a 1:1 mixture of 20% sucrose/PBS and optimal cutting temperature compound (OCT) (Fisher HealthCare 4585) overnight. The brains were embedded in OCT, flash-frozen in a mould, stored at -80°C, and cryosectioned at -18°C on a CM1860 cryostat into 12 µm slices.

3.3.6 Antigen retrieval

The cryosectioned slices were washed with 1X PBS in a Coplin jar until the excess OCT around the slices dissolved. The PBS was drained and replaced with sodium citrate buffer (10 mmol/L sodium citrate, 0.05% Tween 20, pH 6.0), and the jar was placed in a pressure cooker on a metal rack with the lid partially screwed on. The cooker was filled with double-distilled water to cover the base of the jars and set to high pressure for 10 minutes. Once completed, the slides were cooled by slowly running tap water into the Coplin jar for 10 minutes.

3.3.7 Immunofluorescent staining

The slides were placed into a sequenza rack and washed with 1X PBS. The antibodies were diluted in antibody solution (0.4% [volume/volume] Triton/PBS, 3% [weight/volume] Bovine Serum Albumin) at 1:200 for Pax6 and 1:100 for Tbr2. 100 µl of antibody solution was added to the slide in the sequenza rack and incubated at 4°C overnight. Three 1X PBS washes were performed, and then 100 µl of the antibody solution containing the appropriate secondary antibody (Invitrogen A21206, 1:500) was added to the slide and incubated for 1 h at room temperature in the dark. The slides were washed three times with 1X PBS and then incubated in a coplin jar for 7 minutes in DAPI working solution (5 µl of DAPI stock [5 mg/mL, 14.3 mmol/L] in 50 mL of PBS). Three 1X PBS washes were performed, and the slides were partially dried and mounted in 200 µl of Mowiol (5.3% (w/v) Mowiol 4-88, 10.4% (v/v) glycerol, and 174 mmol/L Tris-HCl, pH 8.5), then sealed with a coverslip. Image acquisition was performed using the Agilent Biotek Cytation 5 and a Zeiss LSM880 Confocal Microscope, and image analysis was conducted with Fiji/ImageJ (NIH).

3.3.8 Behavioural Testing

When the mice reach 9 weeks of age, they are used for a variety of behavioural tests. These tests were carried out over six days, with a 48-hour rest period between each to avoid carry-over effects. Mice were housed under a reversed 12 h light-dark cycle for 3 days prior to testing, and before tests began, they were habituated to the test room for at least one hour in their home cage. Male and female mice were tested on the same day. Between all habituation, training, and testing, the test area and all objects are cleaned with Prevail (1:40 dilution) to avoid olfactory cues. The first test conducted was the Open Field Test (OFT), followed by the Elevated Plus Maze (EPM) to measure anxiety-like behaviours and locomotion. After we performed the Object Recognition Test (OR) to measure memory, and the Three Chamber Sociability Experiment (TCS) to assess

sociability. All recording and timing were done with the Ethovision Tracking software. The scoring was performed manually by a student who was blind to the genotype and sex of the mouse.

3.3.8.1 Open Field Test (OFT)

The OFT is conducted in an empty square arena (90 cm x 90 cm x 30 cm). Each mouse was placed in a corner facing the wall, and its movements were tracked for 5 minutes and 30 seconds (Fig. 15). Behavioural parameters recorded included time spent in the center zone, distance travelled in the center (defined as the area ≥ 17 cm from the walls), and total distance travelled. Increased time spent near the walls (thigmotaxis) is interpreted as an indicator of anxiety-like behaviour in mice.

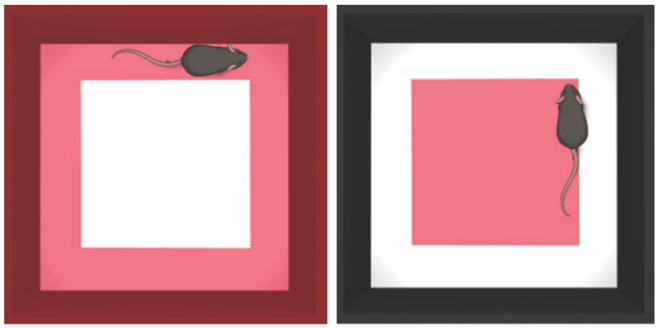

Figure 15: Open Field Test. Representative image of the open field arena. Left panel highlights the outer zone while the right panel highlights the center zone used to quantify anxiety.

3.3.8.2 Elevated Plus Maze (EPM)

The EPM consists of a cross-shaped apparatus elevated above the floor, with four arms (arms from center: 32 × 5 cm, walls: 15cm, elevation 75 cm). Two arms are enclosed by walls, and two are open, lacking side walls. The test mouse was placed at the center of the maze facing the enclosed arm, and its movements were tracked for 5 minutes and 30 seconds (Fig. 16). The number of entries into the open arms, time spent in the open arms, and latency to the first entry into an open arm were recorded. Increased time spent in the enclosed arms is interpreted as increased anxiety-like behaviour in mice.

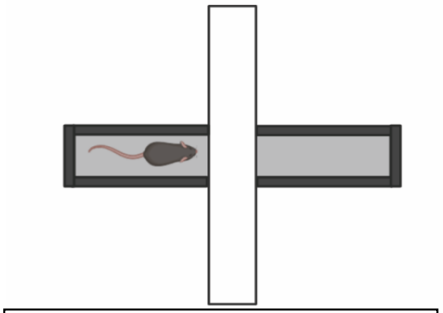

Figure 16: Elevated Plus Maze. Representation of the EPM apparatus showing open and enclosed arms.

3.3.8.3 Object Recognition Test (OR)

The object recognition (OR) test was conducted in the same empty arena (90 × 90 cm) used for the open field test (OFT). Mice were habituated in the empty arena for 5 minutes by being placed in the corner with their heads pointed towards the corner. Immediately following the habituation, two identical objects were placed in opposing corners of the box (Fig. 17), and the mouse was placed in the center of the box with its head pointing towards a corner with no object. The mouse was left with these objects for 3 minutes. 30 minutes after training, one of the objects was replaced with a novel object (Fig. 17). The mouse was placed back in the center of the box and recorded for 5 minutes and 30 seconds. Memory was inferred from the preferential exploration of the novel object compared to the familiar side. The novelty preference was quantified by calculating a discrimination ratio [DR = (novel object exploration – familiar object exploration)/(total object exploration)].

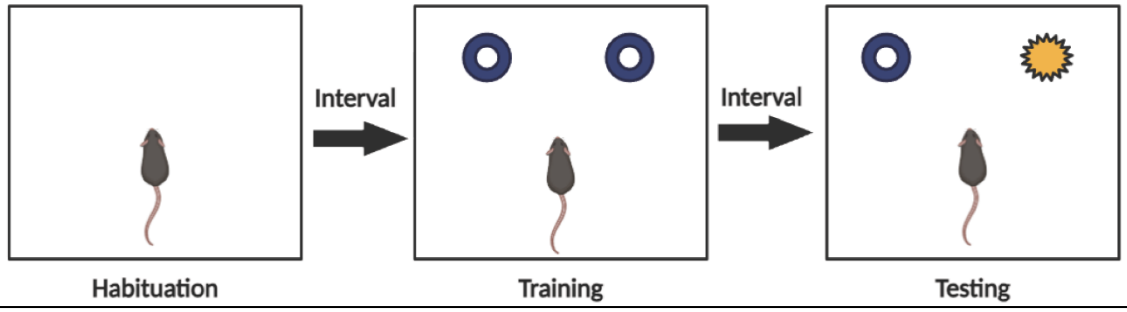

Figure 17: Object Recognition Test. Schematic representation of the three phases of the task: habituation (empty arena), training with 2 identical object, and testing.

3.3.8.4 Three Chamber Sociability Experiment (TCS)

The three-chamber social test (TCS) was conducted in a three-chamber apparatus (39 × 19 cm) with doors connecting the chambers and small wire cages placed in the two side chambers. Prior to the test, the test mice were single-housed for at least two days. Socializing juvenile mice of the same sex of the test mouse were placed in the wired cages in the side chambers (Fig. 18). The test

mouse was placed in the middle chamber with the doors to the side chambers closed for 5 minutes as habituation. Immediately after habituation, the test mouse is returned to the middle chamber, and one door to the socializing mice is opened for the test mouse to interact with for 5 minutes and 30 seconds. Following the training, the door to the unfamiliar mouse was opened, and the test mouse was allowed to interact with the familiar and novel mouse for 5 minutes and 30 seconds. Sociability was inferred from the preferential time spent socializing with the novel mouse as compared to the familiar mouse. The same calculation as the OR were done to get the discrimination ratio.

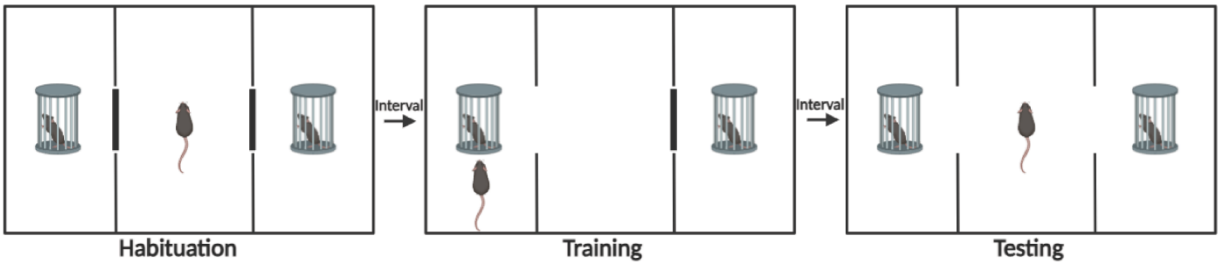

Figure 18: Three Chamber Sociability Experiment. Representative image of the three phases of the task: habituation with test mouse confined to the center chamber, training with access to one side chamber containing a same sex juvenile mouse, and testing with access to both sides chambers.

3.3.9 Statistical Analyses

Analyses were conducted using GraphPad Prism, with independent-samples t tests for single-variable manipulations for two groups, one-way ANOVA for single variable manipulations with more than two groups, and two-way ANOVA for multiple-variable manipulations. When the omnibus test was significant, post hoc analyses were conducted with LSD post hoc or independent samples t-tests when appropriate. The number of replicates per group is stated in the figure legends, as is data representation. Significance was set at $p < 0.05$. Significant outliers were identified using Grubbs's test for outliers in GraphPad Prism.

3.4 Results

3.4.1 Generation and Validation of a Cortex-Specific Conditional Knockout Mouse

As *Srcap* null mice are embryonic lethal at E9.5[3], we generated a conditional knockout mouse model to delete *Srcap* specifically in the developing dorsal telencephalon. To do so, *Srcap*$^{fl/fl}$ mice, in which exon 7 is flanked by LoxP sites, were crossed with Emx1^{Cre} mice. Because Emx1 is expressed in cortical neural progenitors beginning around E10.5, this strategy enabled cortex-specific deletion of *Srcap* during neurogenesis while avoiding the early embryonic lethality associated with global *Srcap* loss.

After generating *Srcap* cKO and *Srcap* cHet, we validated the efficiency of *Srcap* deletion in the cortex. Western blot analysis of P21 cortical lysates demonstrated a robust loss of Srcap protein in the *Srcap* cKO samples, with the remaining signal likely originating from the non-Emx1-expressing cell populations (Fig. 19A). P21 lysates were used rather than embryonic ones due to embryonic cortices not providing enough material to reliably conduct Western blot analysis. To further confirm the ablation efficiency specifically in embryonic tissues, we performed qPCR targeting exon 7 of *Srcap* in E17.5 cortices. This analysis showed a clear reduction in *Srcap* mRNA in both *Srcap* cHet and cKO embryos (Fig. 19B).

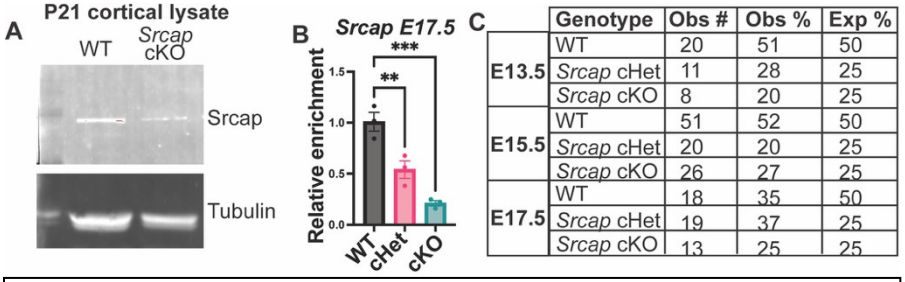

C

	Genotype	Obs #	Obs %	Exp %
E13.5	WT	20	51	50
	Srcap cHet	11	28	25
	Srcap cKO	8	20	25
E15.5	WT	51	52	50
	Srcap cHet	20	20	25
	Srcap cKO	26	27	25
E17.5	WT	18	35	50
	Srcap cHet	19	37	25
	Srcap cKO	13	25	25

Figure 19: Validation of Srcap cKO mouse. (A) Western blot from P21 WT and *Srcap* cKO brains showing ablation of Srcap protein. **(B)** qPCR was used to measure the change in gene expression in E17.5 cortex from WT, *Srcap* cHet, and *Srcap* cKO mice. The relative expression was normalized to housekeeping genes Gapdh and ActB. Data are expressed as mean ± SEM. Two-way ANOVA *p < 0.05. **(C)** Number of mice obtained at E13.5, E15.5, and E17.5 displaying mendelian numbers.

To determine whether *Srcap* ablation in the developing cortex affects embryonic viability, we also quantified the number of embryos obtained at 3 different developmental stages for each genotype. The distribution of genotypes followed the expected Mendelian ratios, indicating that *Srcap* ablation does not cause embryonic lethality (Fig. 19C). However, *Srcap* cKO mice display poor postnatal health and require euthanasia by P21.

3.4.2 Cortex-Specific *Srcap* deletion Disrupts Cortical Morphogenesis

Given the role of H2A.Z in cortical development[7,8], and the association of *SRCAP* mutations with cortical abnormalities in NDDs, we next investigated whether loss of *Srcap*, alters cortical architecture. To this end, we quantified ventricular area, cortical area, and cortical thickness in control, *Srcap* cHet, and *Srcap* cKO mice.

DAPI staining of coronal brain sections from E15.5 embryos revealed that *Srcap* cKO brains exhibited significantly reduced total cortical area and thickness compared to controls (Fig 20 A-B,E). To determine whether these structural abnormalities were associated with altered cellular content, we quantified total cortical cell number at E15.5. This analysis revealed a significant reduction in cell number in *Srcap* cKO embryos (Fig. 20C). These findings indicate that Srcap regulates cortical development, with complete loss leading to reduced cellular content and severe structural defects.

In addition to cortical defects, we also observed altered ventricular morphology (Fig. 20E). Quantification revealed a significant reduction in *Srcap* cKO compared with control mice (Fig. 20D). Together, these results indicate that loss of *Srcap* is associated with structural abnormalities in both ventricular and cortical architecture.

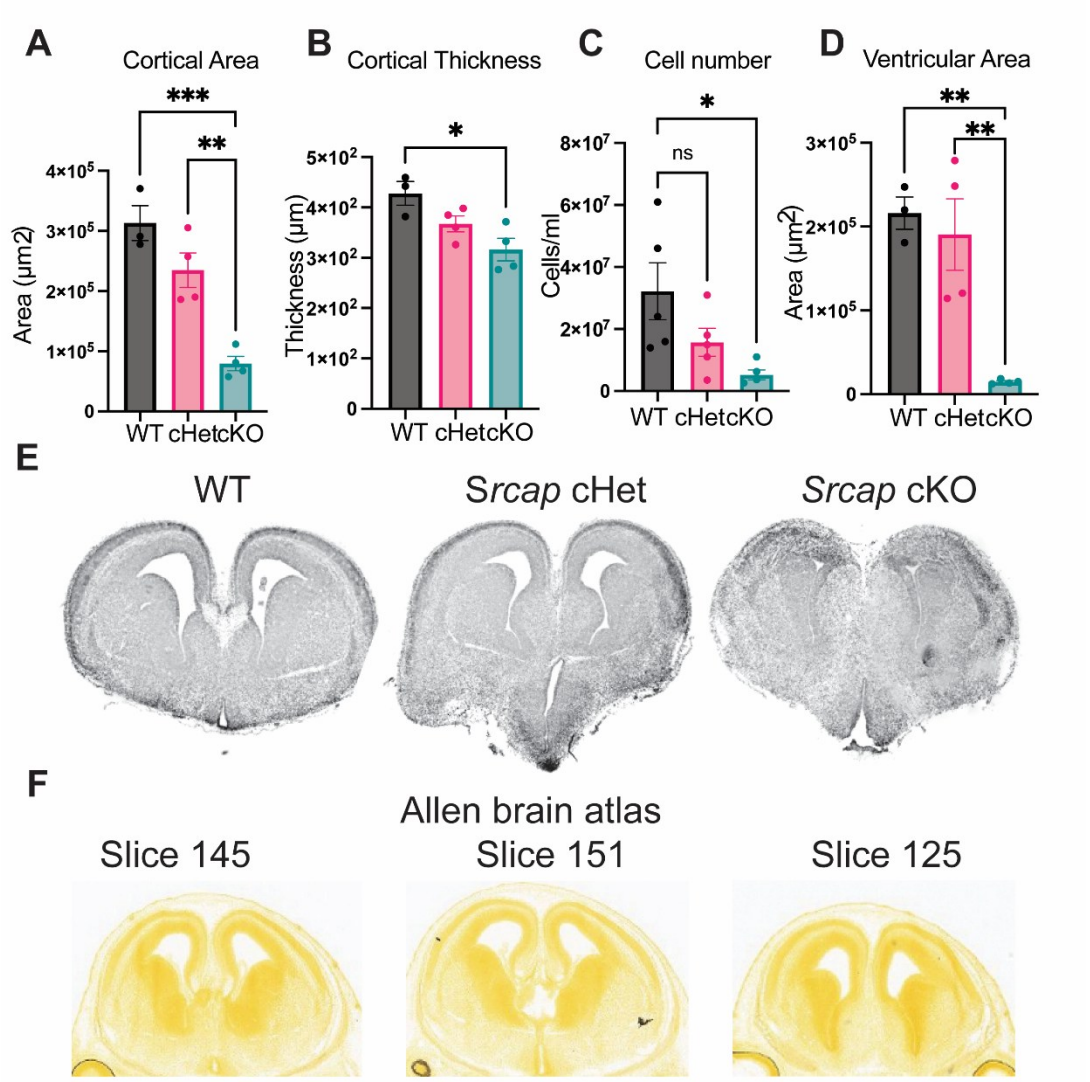

Figure 20: Cortex-specific Srcap deletion disrupts cortical morphogenesis. (A-D) Quantification of cortical area **(A)** cortical thickness **(B)**, total cortical cell number **(C)**, and ventricular area **(D)** at E15.5. **(E)** Representative DAPI-stained coronal brain sections from WT, *Srcap* cHet, and *Srcap* cKO embryos at E15.5. **(F)** Corresponding anatomical reference sections from the Allen Brain Atlas at matched rostrocaudal levels. Data are presented as mean ± SEM. Statistical significance was determined by one-way ANOVA followed by multiple comparisons; *p < 0.05, **p < 0.01, ***p < 0.001; ns, not significant.

3.4.3 *Srcap* Regulates Neural Progenitors Population During Neurogenesis

To determine whether the observed structural abnormalities are associated with altered laminar organization and progenitor populations, we examined the distribution of RGPs and IPCs using Pax6 and Tbr2 immunostaining, respectively (Fig. 21). Pax6 is a transcription factor that is highly expressed in RGPs within the VZ[9] and Tbr2 is expressed in IPCs within the SVZ[10] of the developing cortex. Analysis of fluorescence intensity profiles across cortical depth revealed a significant reduction in Pax6 signal in Srcap cKO mice compared to WT (Fig. 21A,C). Two-way ANOVA showed a significant main effect of genotype ($p = 0.0014$), with no significant genotype × cortical depth interaction ($p = 0.91$), indicating that the reduction occurs broadly across the cortex rather than within a specific region. Together, these results suggest a global reduction in RGP-associated signal without altered spatial distribution, consistent with a decrease in progenitor abundance rather than mislocalization.

Analysis of fluorescence intensity profiles across cortical depth revealed a marked reduction in Tbr2 signal in Srcap cKO mice compared to WT (Fig. 21B,D). Two-way ANOVA showed a strong main effect of genotype ($p < 0.0001$), with no significant interaction between genotype and cortical depth ($p = 0.56$), indicating that the reduction occurs broadly across the cortex rather than within a specific region. While the overall intensity profile exhibited variability, including an apical peak likely reflecting Tbr2 antibody cross reacting with Tbr1 (Fig. 21D), the genotype effect remained highly significant. These results indicate a substantial reduction in IPC-associated signal in Srcap cKO mice, suggesting impaired progenitor populations rather than altered spatial distribution.

Together, these findings demonstrate that Srcap loss leads to a global reduction in both RGP and IPC populations without altering their spatial organization, consistent with the reduced cortical cell number and morphological defects observed in Srcap cKO embryos.

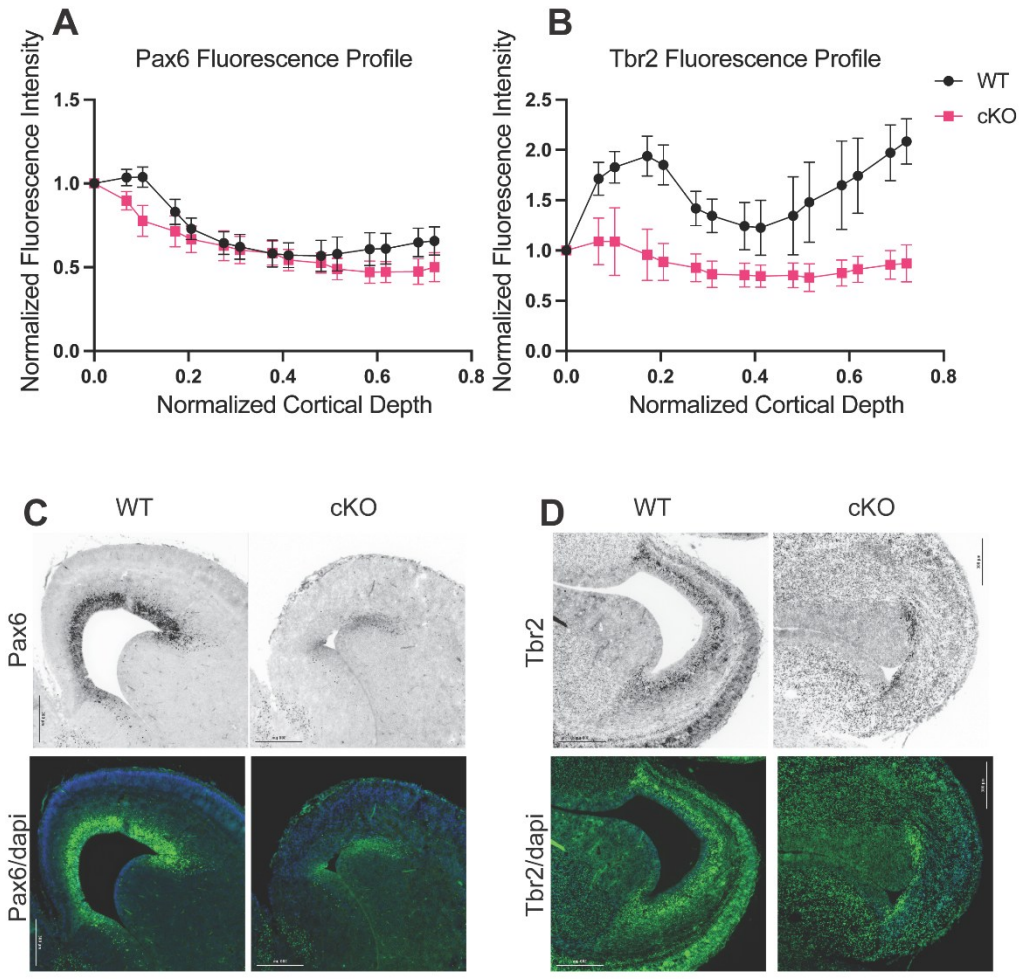

Figure 21: Srcap loss reduces progenitor-associated signals without altering spatial distribution. (A-B) Pax6 **(A)** and Tbr2 **(B)** fluorescence intensity profile across normalized cortical in WT (n = 3) and *Srcap* cKO embryos (n = 3). For Pax6, two-way ANOVA revealed a significant main effect of genotype ($p = 0.0014$) and cortical depth ($p < 0.0001$), with no significant interaction ($p = 0.9105$). For Tbr2, two-way ANOVA revealed a strong main effect of genotype ($p < 0.0001$), with no significant effect of cortical depth ($p = 0.1780$) and no interaction ($p = 0.5641$). Data are presented as mean ± SEM. Fluorescence intensity was quantified across normalized cortical depth (ventricular zone to cortical plate). Reduced signal in both. **(C)** Representative images of Pax6 staining in WT and *Srcap* cKO cortices, with corresponding Pax6/DAPI overlays. **(D)** Representative images of Tbr2 staining in WT and *Srcap* cKO cortices, with corresponding Tbr2/DAPI overlays.

3.4.4 Cortex-Specific Srcap Deletion Alters Adult Behaviour

3.4.4.1 Srcap cHet mice display altered anxiety and exploratory behaviour

Given the pronounced brain morphology phenotype observed in both *Srcap* cKO and cHet mice, we sought to determine whether these structural abnormalities are associated with behavioural alterations. Because *Srcap* cKO mice require euthanasia by P21, behavioural testing was performed in *Srcap* cHet mice.

First, we used the Open Field Test (OFT) (Fig. 22) and the elevated plus maze (EPM) (Fig. 23) to assess anxiety-like behaviours in *Srcap* cHet mice compared to controls. In the OFT, time spent in the center of the arena was not affected by genotype, but a significant main effect of sex was observed, with males spending more time in the center than females (two-way ANOVA, $F(1,53) = 4.47$, $p = 0.0392$; no genotype effect or interaction) (Fig. 22A). This is in accordance with previously published records. While no genotype-dependent differences were observed in time spent in the center, cHet mice exhibited sex-dependent alterations in locomotor activity, (Fig. 22B). Two-way ANOVA revealed a significant interaction between sex and genotype ($F(1,46) = 7.52$, $p = 0.0087$), along with a main effect of sex ($F(1,46) = 21.48$, $p < 0.0001$), but no main effect of genotype. Post hoc comparisons showed that

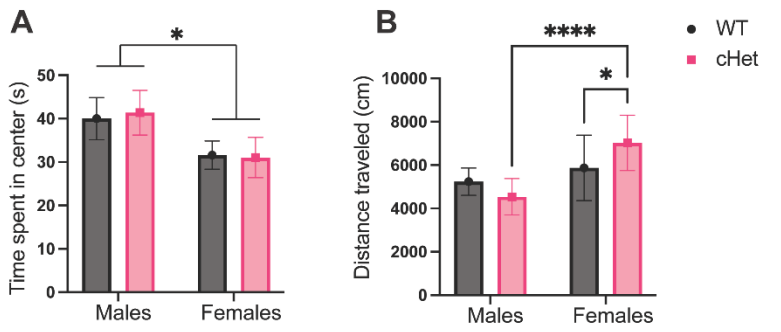

Figure 22: Open field behaviour in WT and cHet mice. The open field test involved male WT (n = 11), male cHet (n = 12), female WT (n = 19), and female cHet (n = 15) mice. **(A)** For time spent in center, two-way ANOVA revealed no main effect of genotype, but a main effect of sex (two-way ANOVA, $F(1,53) = 4.47$, $p = 0.0392$); genotype, $p = 0.9290$; interaction, $p = 0.8275$). **(B)** Total distance travelled revealed a significant sex x genotype interaction (two-way ANOVA: $F(1, 46) = 7.52$, $p = 0.0087$) and a main effect of sex ($F(1,46) = 21.48$, $p < 0.0001$), with no main effect of genotype ($p = 0.5057$). Post hoc comparisons (Sidak's test) showed increased locomotor activity in cHet females compared to WT females and cHet males. Data are presented as mean ± SEM. *$p < 0.05$, **$p < 0.01$, ****$p < 0.0001$.

cHet females exhibited increased distance traveled compared to WT females and cHet males, while cHet males displayed reduced locomotor activity relative to WT males (Fig. 22B). These findings suggest that *Srcap* haploinsufficiency affects exploratory behaviour in a sex specific manner.

In the EPM, *Srcap* cHet spent significantly more time in the open arms than WT mice, regardless of sex (Fig. 23A). Notably, female cHet mice spent significantly more time in open arms than males of the same genotype (Fig. 23A), highlighting significant sex differences in Srcap-related behaviours. A two-way ANOVA revealed significant main effects of genotype and sex, with females spending more time on the open arms than males, and no significant genotype x sex interaction (two-way ANOVA, genotype $F(1,54) = 18.67$, $p < 0.0001$, sex ($F(1,54) = 4.10$, $p = 0.0478$). Similarly, the number of entries into the open arms was increased in cHet mice, as reflected by significant main effects of genotype ($F(1,54) = 9.86$, $p = 0.0027$) and sex ($F(1,54) = 8.43$, $p = 0.0053$), with no significant interaction (Fig. 23B). These findings further support a genotype-dependent increase in exploratory behavior in the open arms. Latency to enter the open arms showed no significant interaction or main effects; however, a trend toward a genotype effect

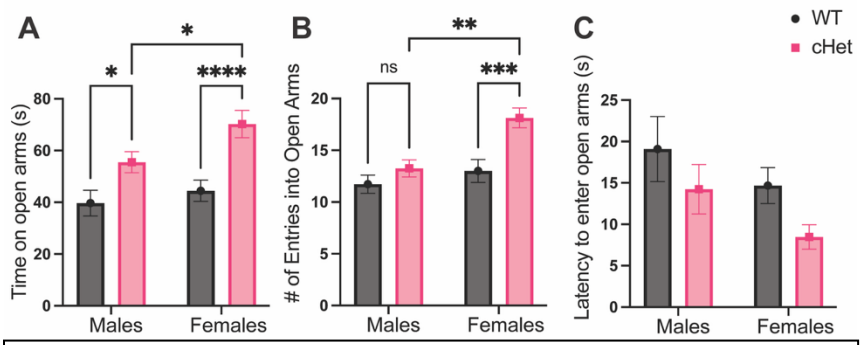

Figure 23: Elevated plus maze behaviour in WT and cHet mice. The elevated plus maze involved male WT (n = 11), male cHet (n = 12), female WT (n = 19), and female cHet (n = 15) mice. **(A)** Time spent in the open arms was increased in cHet mice compared to WT, with significant main effects of genotype (two-way ANOVA: $F(1,54) = 18.67$, $p < 0.0001$) and sex ($F(1,54) = 4.10$, p – 0.0478), and no interaction ($p = 0.0369$). **(B)** Number of entries into the open arms was also increased in cHet mice, with significant main effects of genotype ($F(1,54) = 9.86$, $p = 0.0027$) and sex ($F(1,54) = 8.43$, $p = 0.0053$), and no interaction ($p = 0.0943$). **(C)** Latency to enter the open arms showed no significant effects, although a trend toward a genotype effect was observed ($F(1,49) = 3.94$, $p = 0.0527$). Data are presented as mean ± SEM. *p < 0.05, **p < 0.01, ****p < 0.0001.

was observed (F(1,49) = 3.94, p = 0.0527), with cHet mice exhibiting reduced latency compared to WT (Fig. 23C).

Together, these results indicate that cHet mice display reduced anxiety-like behaviour, characterized by increased open-arm exploration and a tendency toward faster open-arm entry.

3.4.4.2 Srcap haploinsufficiency does not affect memory formation

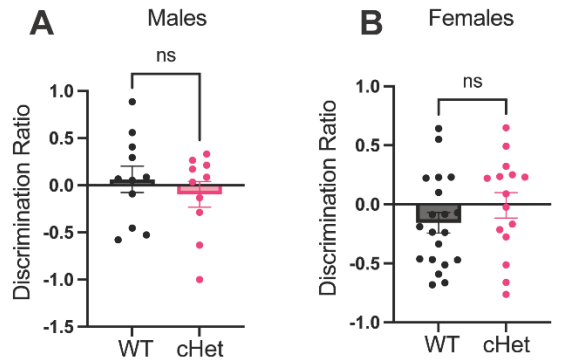

Figure 24: Object location memory performance in WT and cHet mice. The object recognition test involved male WT (n = 11), male cHet (n = 10), female WT (n = 19), and female cHet (n = 15) mice. Discrimination ratio did not differ between WT and cHet mice in either males **(A)** or females **(B)**, indicating no genotype-dependent effect on object location memory. Data are presented as mean ± SEM with individual data points shown. Statistical comparisons were performed using unpaired t-tests within each sex; ns, not significant.

Epigenetic mechanisms, including histone variant dynamics such as H2A.Z incorporation, have been implicated in the regulation of learning and memory[11]. To determine whether *Srcap* haploinsufficiency affects memory-related behaviours, we performed the Object Recognition (OR) test in *Srcap* cHet mice compared with WT controls. Object location memory was assessed using the discrimination ratio. No significant differences were observed between genotypes in either males or females (Fig. 24A-B). Both WT and cHet mice displayed comparable discrimination ratios, indicating similar performance in spatial memory (Fig. 24). These results suggest that cHet mutation does not impair object location memory under the conditions tested.

3.4.4.3 Sociability remains intact in Srcap cKO mice

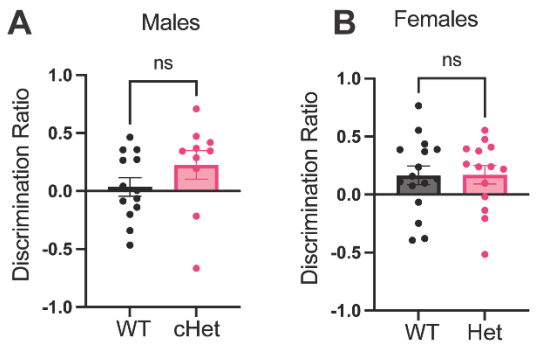

Figure 25: Three-chamber sociability test in WT and cHet mice. Discrimination ratio did not differ between WT and cHet mice in either males **(A)** or females **(B)**, indicating no genotype-dependent effect on sociability. Data are presented as mean ± SEM with individual data points shown. Statistical comparisons were performed using unpaired t-tests within each sex; ns, not significant.

Social interaction deficits are a common feature of several neurodevelopmental disorders and are frequently assessed in mouse models using the Three Chambers Test (TCS). No significant differences in discrimination ratio were observed between WT and cHet mice in either males or females (Fig. 25A-B). Both genotypes displayed comparable preference for the social stimulus, indicating intact sociability. These results suggest that cHet mutation does not impair social behavior under the conditions tested.

3.5 Discussion

As compared to *in vitro* cell models, *in vivo* mouse models allowed us to look at the effects of Srcap loss in the highly complex environment of the developing cortex and reveal structural and behavioural consequences. Our work reveals that Srcap has a crucial role in cortical development. Srcap loss affected cortical and ventricular morphology and prevented proper laminar specification. In adult mice, these abnormalities contributed to altered behavioural outcomes.

3.5.1 Srcap is an important regulatory of cortical development

Our work demonstrates that the cortex-specific deletion of *Srcap* leads to significant structural abnormalities during corticogenesis. Notably, *Srcap* cKO embryos exhibited reduced cortical area (Fig. 20A) decreased cortical thickness (Fig. 20B), and reduced total cortical cell number (Fig.

20C). These phenotypes indicate a fundamental disruption of neural progenitor biology. The developing cortex relies on the expansion and maintenance of RGPs and IPCs, which together generate the neuronal populations required for proper cortical architecture[12]. Consistent with this, we observed a significant reduction in total cortical cell number in *Srcap* cKO embryos, accompanied by a global decrease in both $Pax6^+$ RGP (Fig. 21A) and $Tbr2^+$ IPCs (Fig. 21B). These findings indicate that Srcap is required to maintain progenitor populations during neurogenesis and suggest that impaired progenitor proliferation and/or maintenance underlie the observed reduction in cortical size. Future studies will investigate the cellular mechanisms underlying this phenotype by assessing proliferation and survival using BrdU incorporation and Ki67 staining, and apoptosis using TUNEL assays. In parallel, we will examine markers of cortical layer specification (e.g., Ctip2, Satb2, and Pou3f2) to determine whether Srcap loss also impairs neuronal differentiation and laminar organization. Together, these approaches will allow us to distinguish whether the observed reduction in cortical size arises primarily from defects in progenitor proliferation, increased cell death, or altered differentiation and cortical architecture.

3.5.2 Srcap function could be linked to RGP polarity

Importantly, the structural defects also include significant alterations in ventricular morphology (Fig. 20D). The ventricular zone (VZ), which lines the lateral ventricles, is composed of highly polarized RGPs that maintain apical contact with the ventricular surface[13]. The observed reduction in ventricular area in *Srcap* cKO embryos likely reflects, at least in part, the decreased number of progenitors, as fewer apically anchored cells would contribute to a reduced ventricular surface and altered cortical geometry. However, ventricular morphology is also influenced by the structural organization and polarity of the VZ. RGPs exhibit pronounced apical-basal polarity, maintained through adherens junctions[14] and cytoskeletal organization, which are essential for preserving

tissue integrity, coordinating interkinetic nuclear migration, and regulating the balance between symmetric and asymmetric divisions[15]. Disruption of progenitor polarity or apical adhesion has been shown in multiple mouse models to result in ventricular abnormalities, including narrowing, deformation, or collapse of the ventricular space, often accompanied by VZ disorganization and progenitor delamination[16,17]. In this context, the ventricular phenotype observed upon *Srcap* loss may reflect not only reduced progenitor numbers but also impaired maintenance of VZ architecture.

3.5.3 Dose-dependent effect of Srcap

Notably, though *Srcap* cHet mice did not show a significant reduction compared to the WTs in their, they consistently showed an intermediate trend. This pattern could indicate a dose-dependent role for *Srcap* in cortical development where partial loss of function produces subtle or context-dependent effects. This is particularly relevant in the context of human disease, as all known pathogenic *SRCAP* mutations are heterozygous, suggesting that partial loss of function may underlie subtle but functionally relevant phenotypes. However, mutations in different part of the *SRCAP* gene have been shown to cause clinically distinct diseases. This led to speculate that different mutations can have different effects, with some generating dominant negative mutants and others leading to haploinsufficiency. Our work confirms that Srcap dosage is important and leads to different phenotypic outcomes.

3.5.4 Srcap dysfunction contributes to abnormal anxiety-related and exploratory behaviours

In addition to developmental defects, we observed behavioural alterations in *Srcap* cHet mice, particularly in anxiety-related behaviours, while memory and sociability remained largely intact. Notably, while the OFT (Fig. 22A) did not show any genotype-related difference in anxiety, the

EPM revealed reduced anxiety-like behaviour in cHet mice, with female cHet mice showing a significant reduction even relative to the male cHet mice (Fig. 23A-B). Although the OFT and EPM are both commonly used to assess anxiety-like behaviour, their results do not always align[18]. Comparative studies indicate that EPM imposes a stronger approach-avoidance conflict than the OFT, as the open arms are both elevated and exposed, making the environment more stressful than the center of the open field[19]. As a result, the EPM may be more sensitive to changes in risk assessment and in the avoidance of exposed spaces, whereas the OFT is more strongly influenced by exploratory drive and locomotor activity[18]. One possible interpretation is that the genotype effect in cHet mice was insufficient to alter general center exploration in the OFT, but became apparent under the more aversive conditions of the EPM. The OFT also revealed increased locomotor activity in female cHet mice relative to female WT and male cHet mice (Fig. 22B). This is important because altered locomotion can influence the interpretation of anxiety-related behaviour, particularly in assays that rely on exploratory choices[18,20]. In the EPM, female cHet mice consistently showed reduced anxiety-like behaviour relative to male cHet mice (Fig. 23A-B), even though females spent less time in the center than males in the OFT (Fig. 22A). This raises the possibility that part of the EPM phenotype in female cHet mice may reflect increased exploratory drive rather than reduced anxiety alone. The increase in exploratory drive could be indicative of the female mice having hyperactive, as ADHD is a NDD that is associated with SRCAP dysfunction in humans[21].

Along with anxiety-like behaviour, we assessed memory (Fig. 24) and sociability (Fig. 25), but did not detect differences between genotypes or sexes in either domain. NDDs are commonly associated with impairments across multiple behavioural domains, including anxiety[22], memory[23], and sociability[24]. However, these outcomes were not broadly reproduced in our mouse model. This

may reflect the nature of the Srcap mutation used here. In the present study, behavioural analyses were restricted to cortex-specific *Srcap* cHet mice because cKO animals are postnatally lethal. While this approach allowed us to assess the functional consequences of *Srcap* haploinsufficiency within the cortex, it does not capture potential contributions from other brain regions or developmental stages. Notably, a recent study using a different *Srcap* heterozygous knockout model reported broader behavioural phenotypes, including anxiety, social, and learning impairments[25]. Future studies will involve crossing $Srcap^{fl/+}$ mice with a CMV-Cre driver to generate a constitutive heterozygous model. This approach will enable the assessment of behavioural phenotypes arising from global *Srcap* haploinsufficiency, providing a more comprehensive understanding of how reduced *Srcap* dosage impacts neural circuit function and behaviour.

3.5.5 Limitations

A major limitation of this project is that the cortex-specific model may not fully capture the phenotypic spectrum of SRCAP-related neurodevelopmental disorders. Pathogenic SRCAP variants in patients differ in both type and location, and these differences are associated with distinct phenotypic outcomes. As a result, our mouse model may only capture part of the underlying human disease biology. In addition, this model does not account for developmental abnormalities that may arise from global impairment of Srcap function earlier in development. Because disruptions during early developmental processes can have major downstream consequences, the absence of early developmental Srcap loss in our model may reduce the severity or breadth of the phenotypes observed in our mice. However, this model was designed to investigate the role of Srcap in cortical neurodevelopment rather than to fully recapitulate SRCAP-

related disorders. In this regard, it provides an important advantage by limiting potential confounding effects of Srcap loss outside the cortex.

3.5.6 Conclusions

This study shows that Srcap function is needed in the cortex during development and that this loss results in both structural and behavioural abnormalities. When Srcap loss occurs in the developing mouse cortex, it leads to altered ventricular and cortical morphology, consistent with impaired cortical development. These structural abnormalities are accompanied by selective changes in anxiety-like and exploratory behaviours, although the behavioural phenotype differs from that typically observed in patients with SRCAP-related neurodevelopmental disorders. This divergence suggests that the timing, spatial restriction, and conditional nature of Srcap loss in our model may contribute to the distinct phenotypic outcome. Taken as a whole, these findings reveal an essential role of Srcap regulation to support proper progenitor function, cortical development, and downstream behavioural outcomes.

3.6 Acknowledgements

This research was supported by an NSERC Discovery Grant, NSERC Discovery Accelerator Supplement to GS.

3.7 References

1. Goffinet AM. *Mouse Brain Development*. (Springer-Verlag, Berlin, 2000).
2. Zoltán Molnár *et al.* Comparative aspects of cerebral cortical development. *Eur J Neurosci* **23**, 921–34 (2006).
3. Ye, B. *et al.* The chromatin remodeler SRCAP promotes self-renewal of intestinal stem cells. *EMBO J* **39**, e103786 (2020).
4. Stoner, R. *et al.* Patches of disorganization in the neocortex of children with autism. *N Engl J Med* **370**, 1209–1219 (2014).
5. Gorski, J. *et al.* Cortical excitatory neurons and glia, but not GABAergic neurons, are produced in the Emx1-expressing lineage. *J Neurosci* **22**, 6309–14 (2002).
6. Ramzan, F. *et al.* Sex-specific effects of the histone variant H2A.Z on fear memory, stress-enhanced fear learning and hypersensitivity to pain. *Sci Rep* **10**, 14331 (2020).
7. Shen, T. *et al.* Brain-specific deletion of histone variant H2A.z results in cortical neurogenesis defects and neurodevelopmental disorder. *Nucleic Acids Res* **46**, 2290–2307 (2018).
8. Karanveer S Johal, Sandra A Youssef, & Samira M Ibrahim. Srcap loss alters H2A.Z-dependent and neuronal differentiation-related gene expression in N2A cells. *Biochem Cell Biol* **103**, 1–12 (2025).
9. Martine Manuel *et al.* Pax6 limits the competence of developing cerebral cortical cells to respond to inductive intercellular signals. *PLoS Biol* **20**, E3001563 (2022).
10. Robert F Hevner. Intermediate progenitors and Tbr2 in cortical development. *J Anat* **235**, 616–625 (2019).
11. Samantha D Creighton, Gilda Stefanelli, Anas Reda, & Iva B Zovkic. Epigenetic Mechanisms of Learning and Memory: Implications for Aging. *Int J Mol Sci* **21**, 6918 (2020).
12. Robert Beattie & Simon Hippenmeyer. Mechanisms of radial glia progenitor cell lineage progression. *FEBS Lett* **591**, 3993–4008 (2017).

13. Brian M Howard *et al.* Radial Glia Cells in the Developing Human Brain. *Neuroscientist* **14**, 459–473 (2008).

14. Valeria Viola, Kaviya Chinnappa, & Fiona Francis. Radial glia progenitor polarity in health and disease. *Front Cell Dev Biol* **12**, 1478283 (2024).

15. Lenin Veeraval, Conor J O'Leary, & Helen M Cooper. Adherens Junctions: Guardians of Cortical Development. *Front Cell Dev Biol* **8**, 6 (2020).

16. Anjen Chenn & Christopher A Walsh. Increased neuronal production, enlarged forebrains and cytoarchitectural distortions in beta-catenin overexpressing transgenic mice. *Cereb Cortex* **13**, 599–606 (2003).

17. Kei-ichi Katayama *et al.* Loss of RhoA in neural progenitor cells causes the disruption of adherens junctions and hyperproliferation. *Proc Natl Acad Sci U S A* **108**, 7607–7612 (2011).

18. Mariah Mesquita de Figueiredo Cerqueira *et al.* Comparative analysis between Open Field and Elevated Plus Maze tests as a method for evaluating anxiety-like behavior in mice. *Heliyon* **9**, e14522 (2023).

19. Walf, A. A. & Frye, C. A. The use of the elevated plus maze as an assay of anxiety-related behavior in rodents. *Nat Protoc* **2**, 322–8 (2007).

20. Sinem Gencturk & Gunes Unal. Rodent tests of depression and anxiety: Construct validity and translational relevance. *Cogn Affect Behav Neurosci* **24**, 191–224 (2024).

21. Rots, D. *et al.* Truncating SRCAP variants outside the Floating-Harbor syndrome locus cause a distinct neurodevelopmental disorder with a specific DNA methylation signature. *Am J Hum Genet* **108**, 1053–1068 (2021).

22. Xiaoyun Zhou *et al.* Associations between multiple neurodevelopmental disorders and mental health in children. *J Affect Disord* **393**, 120397 (2026).

23. Ciara J Molloy, Ciara Quigley, Áine McNicholas, Linda Lisanti, & Louise Gallagher. A review of the cognitive impact of neurodevelopmental and neuropsychiatric associated copy number variants. *Transl Psychiatry* 116 (2023) doi:10.1038/s41398-023-02421-6.

24. Emma M Jaisle, Nicole B Groves, Katie E Black, & Michael J Kofler. Linking ADHD and ASD Symptomatology with Social Impairment: The Role of Emotion Dysregulation. *Res Child Adolesc Psychopathol* **3**, 3–16 (2022).

25. Ding, C. *et al.* Srcap haploinsufficiency induced autistic-like behaviors in mice through disruption of Satb2 expression. *Cell Rep* **43**, 114231 (2024).

Chapter 4: Discussion

4.1 Summary of Work

Neurodevelopment requires precise temporal and spatial control of gene expression, and disruption of chromatin regulation is increasingly recognized as a central mechanism underlying NDDs. In this study, we investigated the role of the chromatin remodeler Srcap in regulating cortical development and behaviour. By combining *in vitro* and *in vivo* approaches, we demonstrate that Srcap is a critical regulator of neurodevelopment, acting by modulating H2A.Z dynamics to control gene expression, progenitor populations, and cortical architecture.

Our work in N2A cells established that Srcap is required for proper H2A.Z deposition at neurodevelopmental and activity-dependent genes. Loss of Srcap resulted in reduced H2A.Z occupancy and disrupted its accumulation during retinoic acid-induced differentiation of N2A, leading to altered expression of genes involved in neuronal development and function. Importantly, these effects occurred independently of CBP recruitment or global histone acetylation, indicating that Srcap exerts a specific role in regulating H2A.Z-mediated chromatin remodeling. Together, these findings support a model in which Srcap governs the dynamic redistribution of H2A.Z required for proper transcriptional transitions during neuronal differentiation.

Extending these findings *in vivo*, we found that loss of *Srcap* in the developing cortex impaired cortical development and contributed to abnormal adult behaviours. Specifically, loss of Srcap altered cortical and ventricular morphology, reduced cortex cell number, and affected progenitor populations. Analysis of behavioural data revealed that *Srcap* cHet mice were less anxious than WT mice and cHet females also having an increase in exploratory drive. Taken together, these results implicate Srcap as an important regulator of cortical development whose lack of function contributes to behavioural changes in adults.

4.2 Combining *in vitro* and *in vivo* data

Our *in vivo* findings can be linked to Srcap's role in regulating H2A.Z dynamics during developmental gene expression. H2A.Z is known to be dynamically redistributed during differentiation, being removed from genes that become inactive and enriched at genes that become active. Our *in vitro* data indicate that Srcap loss disrupts this dynamic process, preventing proper transcriptional reprogramming. In our *in vitro* studies, three neurodevelopmental genes were studied, *Nr4a2*, *Sox5*, and *Fezf2*. NR4A2 is a transcription factor with a critical role in the differentiation, development, and survival of dopaminergic neurons[1]; SOX5 is a transcription factor that regulates cell cycle and cell fate[2], and FEZF2 regulates the specification of telencephalic progenitors[3]. In the developing cortex, the disruption caused by the loss of Srcap would be expected to impair the timely activation of these and other genes required for progenitor proliferation, differentiation, and neuronal migration[4]. Thus, the defects observed in *Srcap* cKO embryos likely reflect a failure to properly execute developmental transcriptional programs due to impaired chromatin remodeling.

The altered behaviour of the *Srcap* cHet mice could be due to the cortical defects that occur during development. While they did not show a significant difference from the WT when looking at the morphological characteristics we measured individually, they consistently had an intermediate trend, which could mean that taken together, the cHets could be different from the WT.

4.3 Fulfillment of Thesis Aims

4.3.1 How Srcap regulates H2A.Z incorporation during neuronal differentiation and how its loss alters developmentally important gene expression programs.

In our work using N2A cells, we showed that Srcap plays an important role in incorporating H2A.Z into chromatin (Fig. 7). When differentiation occurs, there is an initial removal of H2A.Z at various sites across the genome (Fig. 9). As differentiation progresses, there is an increase in H2A.Z levels (Fig. 10). However, both the initial removal and subsequent reincorporation are impaired when Srcap is knocked down. This suggests that Srcap is needed to regulate H2A.Z dynamics during the differentiation process. H2A.Z has a variety of effects on transcription, acting as either an active[9] or repressive[10] marker of transcription, while also mediating activity-dependent gene induction[11]. Therefore, the dysregulation of H2A.Z dynamics during cell differentiation would result in a dysregulation of gene expression. Indeed, we observed altered expression of H2A.Z bound genes in the absence of Srcap (Fig. 11B). While we observe that several genes display similar expression levels compared to controls after 72h of differentiation (Fig. 11C), at 24 hours we showed profound alterations in gene expression (Fig. 11B). As cortical development is a time-sensitive process, these time-dependent alterations may result in big impairments during development.

4.3.2 Examine the impact of Srcap loss during corticogenesis on neural progenitor specification and neuronal differentiation within the developing cortex.

The generation of a conditional knockout mouse model for Srcap allowed us to investigate the impact of its loss in cortical architecture.

First, we focused on assessing the morphological characteristics of the cortex, as they displayed a visible and marked phenotype. Our measurements revealed a reduction in the cortical area (Fig. 20A), cortical thickness (Fig. 20B), cell number (Fig. 20C), and ventricular area (Fig. 20D). Overall, these findings suggest that Srcap is necessary to regulate cortical morphogenesis and indicate that a reduced neuronal output may be present when Srcap is knocked out.

To investigate if there is an impairment in the progenitor population, We performed immunofluorescence stainings for Pax6 and Tbr2 to label RGPs and IPCs respectively. In mice, RGPs and IPCs make up the major progenitor populations that generate the neurons on the cortex. If these populations are affected, then this would result in large downstream changes in cortical structure. The fluorescence profile analysis of these markers across cortical depth revealed a reduction in both Pax6+ cells (Fig. 21A) and Tbr2+ cells (Fig. 21B), indicative of a depletion of the progenitor population. Though the cause of the depletion is still unknown, the presence of the depletion indicates that Srcap is needed for the maintenance of the progenitor populations.

4.3.3 Assess whether disruption of Srcap-dependent chromatin regulation during cortical development leads to long-term behavioural alterations relevant to neurodevelopmental disorders.

While our work in embryos could use animals that lack one or both copies of *Srcap*, the behavioural characterization was carried out exclusively in Srcap cHet mice, as the KO animals either die or need to be euthanized by P21.

We performed a variety of tests and revealed two significant behavioural differences between the WT and *Srcap* cHet mice. First, Srcap cHet display a reduction in anxiety-like behaviours in the elevated plus maze (Fig. 23). This was accompanied by an increase in exploratory behaviours (Fig. 22B) in the female cHets compared to female WT and male cHets.

Previous work has strongly linked SRCAP dysfunction in ASD[13]. For this reason, we expected the ablation of the Srcap to increase the anxiety of the mice, rather than a decrease. In general, we expected to observe more marked behavioural differences. Importantly, our model is driven by $Emx1^{Cre}$, which ablates *Srcap* expression only in excitatory neurons, leaving inhibitory neurogenesis intact. This could limit our behavioural observations. In addition, different mutations in SRCAP have been linked to the development of clinically distinct diseases, indicating that the loss of only one allele of *Srcap* may not be sufficient to highlight the behavioural abnormalities we were expecting.

4.4 Contribution to Scientific Knowledge

Overall, our findings identify Srcap as an important regulator of H2A.Z deposition and show that loss of Srcap disrupts the dynamics of H2A.Z incorporation and neurodevelopmental gene expression. In addition, this thesis provides a model for investigating the role of Srcap in corticogenesis under both haploinsufficient and complete-knockout conditions, while limiting the confounding effects from Srcap loss outside the cortex.

Previous work has shown that SRCAP dysfunction is a major contributor of a variety of different NDDs [14–17], and there has been plenty of evidence which suggests that Srcap regulates developmental gene expression through H2A.Z incorporation. However, there has not been any research which provide evidence of Srcap's role in neurodevelopment and connect that role with its function of incorporating H2A.Z into the chromatin. In this thesis, we show that Srcap has an important role in neurodevelopment, and that when its function of incorporating H2A.Z is disrupted, this alters neurodevelopmental gene expression.

While other studies have investigated the function of Srcap in neurodevelopment, their models knock out Srcap constitutively, and as such, they can only look at heterozygous mice which

experience haploinsufficiency[18]. As our model uses a Cre-LoxP system to induce the knockout in RGPs, we can investigate corticogenesis in complete-knockout conditions in addition to haploinsufficiency rather than just under haploinsufficiency. This provides a much broader insight into how Srcap functions as we will be able to determine what effects the complete absence of Srcap will have on chromatin architecture, gene expression, and corticogenesis. In addition, as the knockout is spatially restricted to just the RGPs and their lineage, we can limit the effects that Srcap loss from other regions of the brain can have on the mouse.

Overall, our work begins to elucidate the role of Srcap in neurodevelopment and provides a model by which this work can be expanded. By understanding the molecular mechanisms of Srcap in this context, we can determine how the perturbations caused by SRCAP dysfunction contribute to SRCAP-related neurodevelopmental disorders.

4.5 Future Directions

Moving forward with this project, we will be increasing the time points that we are analyzing for the ventricular and cortical morphology to include E13.5 (early neurogenesis) and E17.5 (late neurogenesis). We will be investigating if the microcephlay that we see in our brains was caused by impaired cell proliferation and/or survival. To distinguish these possibilities, we will use histological staining to quantify the number of cells across corticogenesis. We will use cell cycle markers to evaluate the percentage of cells enter (Ki67+) or actively undergoing (phospho-Histone H3) cell cycle . To see if there is increased cell death, we will assess apoptosis using immunostaining for cleaved caspase-3 and TUNEL assays.

To further define the structural phenotype, cortical layer analysis will be expanded to include additional laminar markers in order to determine whether specific neuronal populations are mislocalized and whether neuronal migration is disrupted. Because altered ventricular

morphology may reflect defects in radial glial progenitor organization, future studies will also assess RGP polarity by staining for apical junction proteins together with RGP markers.

To expand the molecular analysis of Srcap-dependent chromatin regulation, we will be conducting Cleavage Under Target and Tagmentation to see how loss of Srcap impacts H2A.Z accumulation across the genome, and single-nuclei RNA-seq identify cell-type-specific transcriptional changes in the developing cortex.

4.7 References

1. Odila Saucedo-Cardenas *et al.* Nurr1 is essential for the induction of the dopaminergic phenotype and the survival of ventral mesencephalic late dopaminergic precursor neurons. *Proc Natl Acad Sci U S A* **95**, 4013–4018 (1998).
2. Patricia L Martinez-Morales, Alejandra C Quiroga, Julio A Barbas, & Aixa V Morales. SOX5 controls cell cycle progression in neural progenitors by interfering with the WNT–β-catenin pathway. *EMBO Rep* **11**, 466–472 (2010).
3. Zhi-Bo Wang *et al.* Fezf2 Regulates Telencephalic Precursor Differentiation from Mouse Embryonic Stem Cells. *Cereb Cortex* **21**, 2177–86 (2011).
4. Shen, T. *et al.* Brain-specific deletion of histone variant H2A.z results in cortical neurogenesis defects and neurodevelopmental disorder. *Nucleic Acids Res* **46**, 2290–2307 (2018).
5. Iva B Zovkic, Brynna S Paulukaitis, Jeremy J Day, & J David Sweatt. Histone H2A.Z subunit exchange controls consolidation of recent and remote memory. *Nature* **515**, 582–6 (2014).
6. Stefanelli, G. *et al.* Learning and Age-Related Changes in Genome-wide H2A.Z Binding in the Mouse Hippocampus. *Cell Rep* **22**, 1124–1131 (2018).
7. Anas Reda *et al.* Role of the histone variant H2A.Z.1 in memory, transcription, and alternative splicing is mediated by lysine modification. *Neuropsychopharmacology* **49**, pages1285-1295 (2024).
8. Ramzan, F. *et al.* Sex-specific effects of the histone variant H2A.Z on fear memory, stress-enhanced fear learning and hypersensitivity to pain. *Sci Rep* **10**, 14331 (2020).
9. Edwige Belotti *et al.* H2A.Z is dispensable for both basal and activated transcription in post-mitotic mouse muscles. *Nucleic Acids Res* **48**, 4601–4613 (2020).
10. Weronika Sura *et al.* Dual Role of the Histone Variant H2A.Z in Transcriptional Regulation of Stress-Response Genes. *Plant Cell* **29**, 791–807 (2017).
11. Vidya Subramanian, Paul A Fields, & Laurie A Boyer. H2A.Z: a molecular rheostat for transcriptional control. *F1000Prime Rep* **7**, (2015).

12. Marta Florio & Wieland B. Huttner. Neural progenitors, neurogenesis and the evolution of the neocortex Available. in *Development* vol. 141 2182–2194 (The Company of Biologists, 2014).

13. Ivan Iossifov *et al.* The contribution of de novo coding mutations to autism spectrum disorder. *Nature* **515**, 216–221 (2014).

14. Rots, D. *et al.* Truncating SRCAP variants outside the Floating-Harbor syndrome locus cause a distinct neurodevelopmental disorder with a specific DNA methylation signature. *Am J Hum Genet* **108**, 1053–1068 (2021).

15. Iossifov, I. *et al.* The contribution of de novo coding mutations to autism spectrum disorder. *Nature* **515**, 216–21 (2014).

16. Nishioka, M. *et al.* Systematic analysis of exonic germline and postzygotic de novo mutations in bipolar disorder. *Nat Commun* **12**, 3750 (2021).

17. Rebecca L Hood *et al.* Mutations in SRCAP, encoding SNF2-related CREBBP activator protein, cause Floating-Harbor syndrome. *Am J Hum Genet* **90**, 308–13 (2012).

18. Ding, C. *et al.* Srcap haploinsufficiency induced autistic-like behaviors in mice through disruption of Satb2 expression. *Cell Rep* **43**, 114231 (2024).

Chapter 5: Appendix

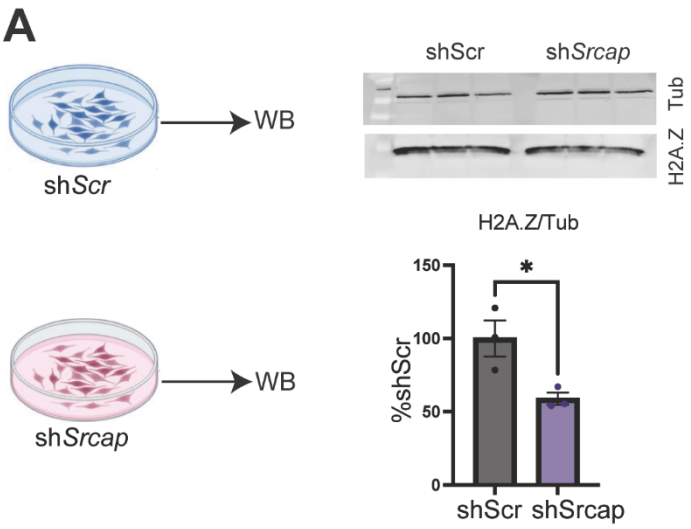

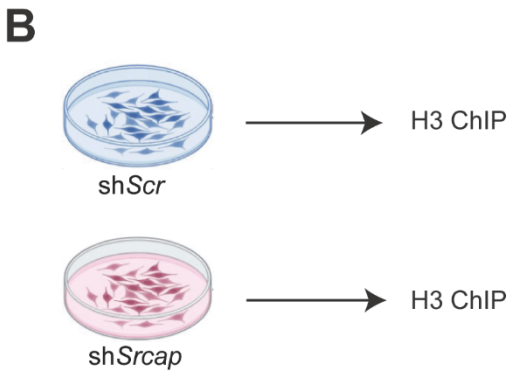

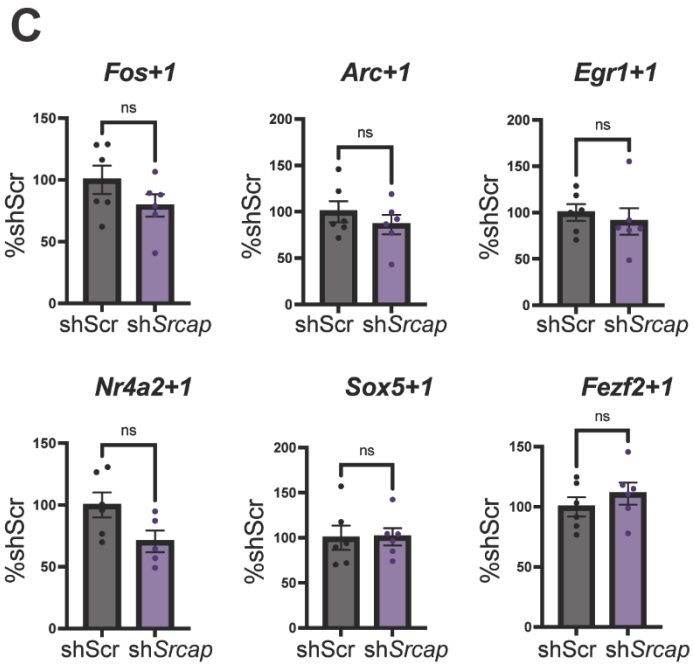

Supplementary Figure 1: Srcap depletion reduces H2A.Za global protein levels but does not alter nucleosome number. (A) Western Blot was used to assess levels of acetylated H2A.Z in N2A cells 48 hours following transfection with sh*Srcap* (n = 3). sh*Srcap* transfection was normalized to shScr transfection. H2A.Z abundance is normalized to tubulin. Data are expressed as mean ± SEM. *p < 0.05. **(B)** Schematic representation of experimental workflow in cultured N2A cells. **(C)** ChIP was used to measure the occupancy of H3 at the first nucleosome (+1 nucleosome) downstream of the transcription start site (TSS) in N2A cells 48 hours following transfection with sh*Srcap* (n=6). *shSrcap* transfection was normalized to shScr transfection. Data are expressed as mean ± SEM. *p < 0.05.

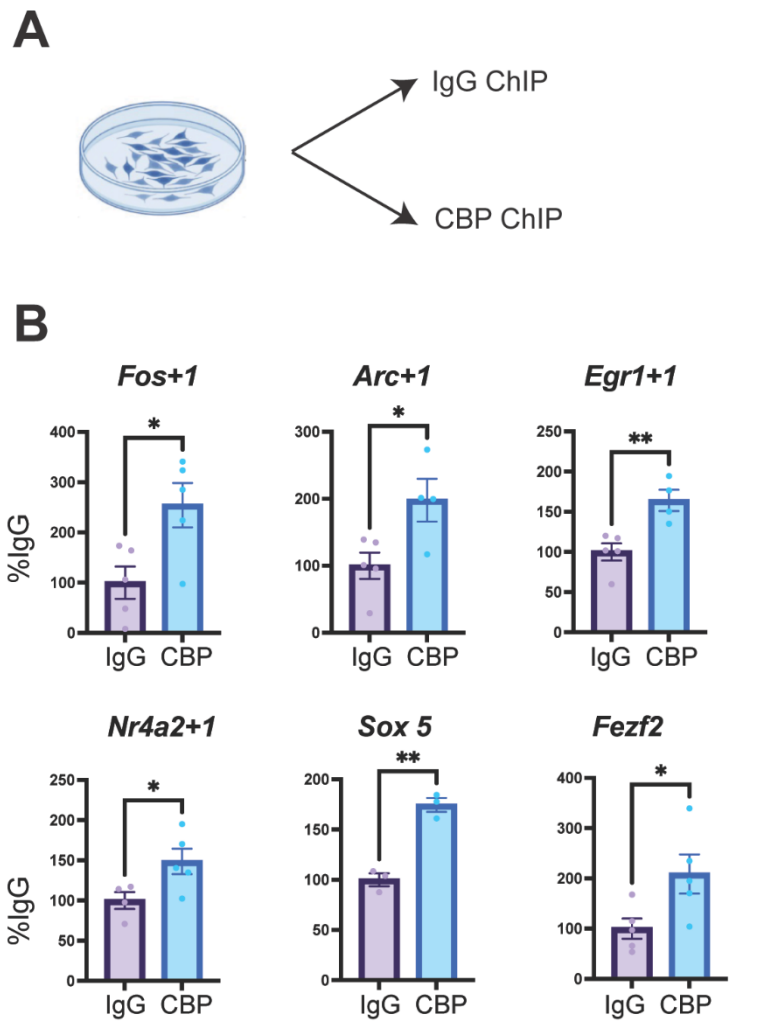

Supplementary Figure 2: CBP is enriched at H2A.Z binding sites. (A) Schematic representation of experimental workflow in cultured N2A cells. **(B)** ChIP was used to measure CBP enrichment at the first nucleosome (+1 nucleosome) downstream of the transcription start site (TSS) in N2A cells compared to IgG. Data are expressed as mean ± SEM. *p < 0.05.

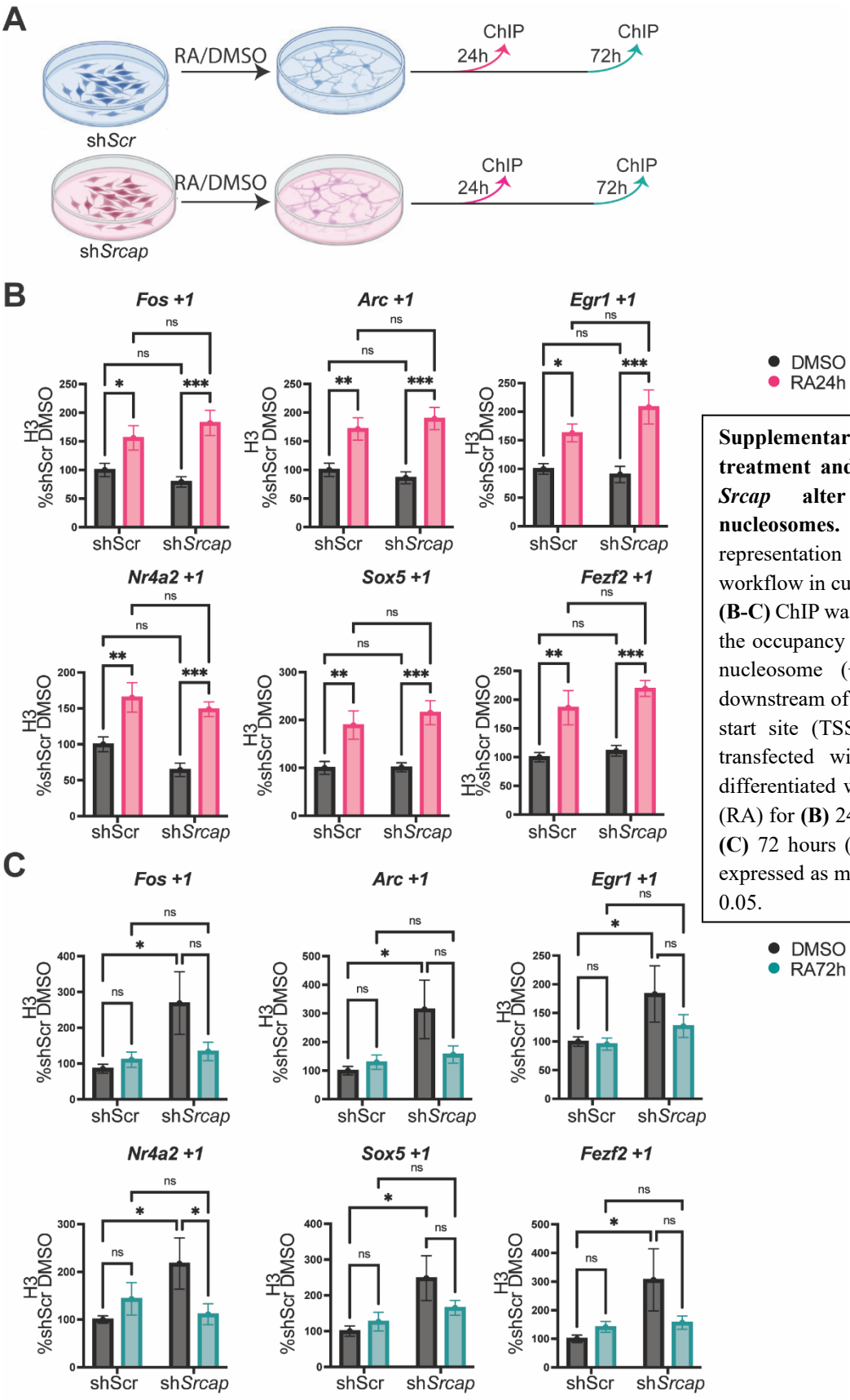

Supplementary Figure 3: RA treatment and knockdown of *Srcap* alter number of nucleosomes. (A) Schematic representation of experimental workflow in cultured N2A cells. **(B-C)** ChIP was used to measure the occupancy of H3 at the first nucleosome (+1 nucleosome) downstream of the transcription start site (TSS) in N2A cells transfected with sh*Srcap* and differentiated with retinoic acid (RA) for **(B)** 24 hours (n = 6) or **(C)** 72 hours (n = 6). Data are expressed as mean ± SEM. *p < 0.05.

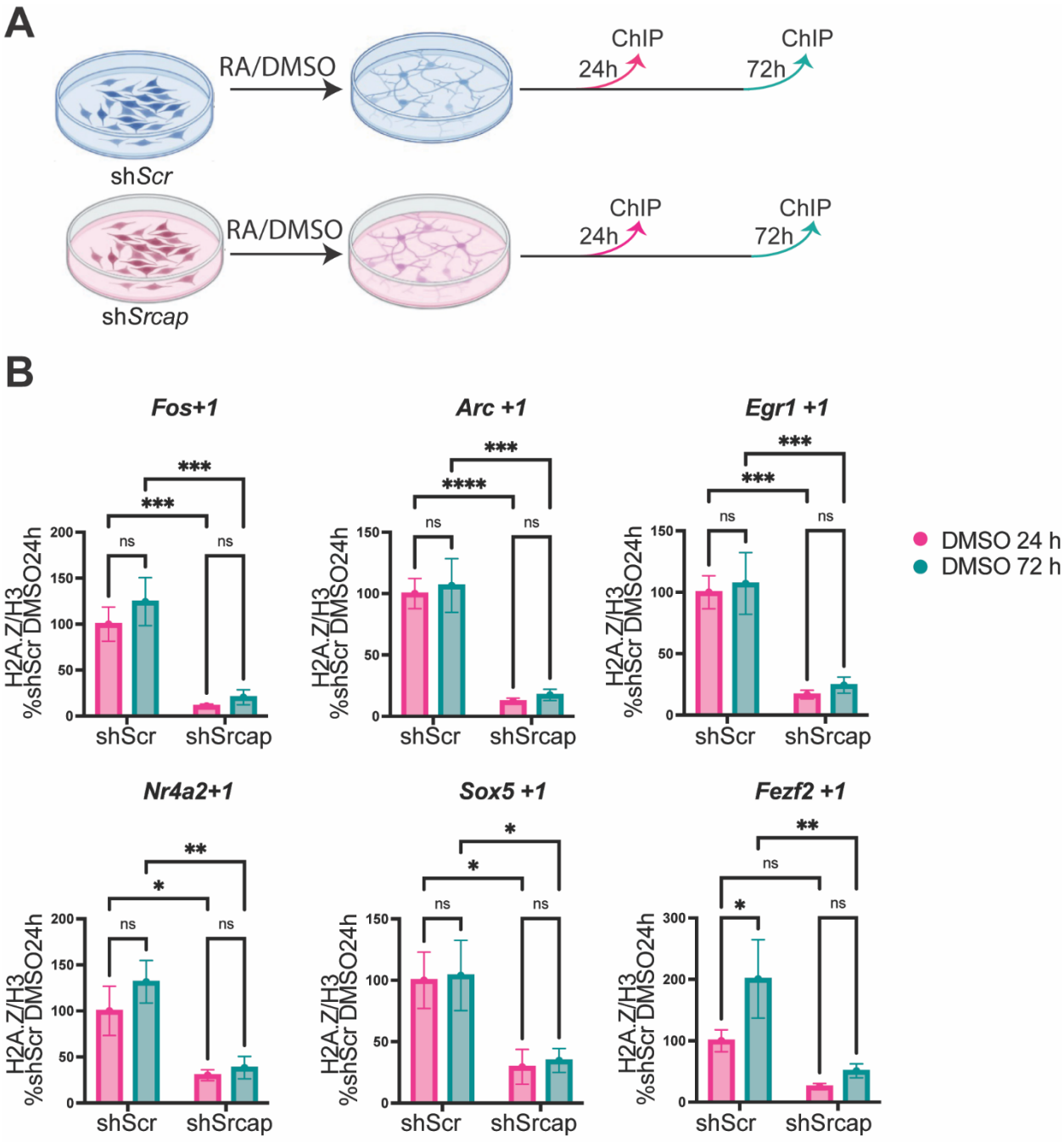

Supplementary Figure 4: Knockdown of *Srcap* reduces abundance of H2A.Z over time. (A) Schematic representation of experimental workflow in cultured N2A cells. **(B)** ChIP data in Figure 3 were re-analyzed to compare H2A.Z occupancy of H2A.Z at the +1 nucleosome between 24 hours (n = 6) and 72 hours (n = 6) after DMSO treatment. H2A.Z abundance is normalized to H3, and data are expressed as % compared to shScr DMSO 24h. Data are expressed as mean ± SEM. Two-way ANOVA *p < 0.05.